AD-A047 194 TEXAS INSTRUMENTS INC DALLAS CENTRAL RESEARCH LABS F/G 20/6
ACTIVE AL(X)GA(1-X)AS DEVICES FOR WAVEGUIDE CIRCUITS.(U)
OCT 77 A R REISINGER , D W BELLAVANCE N00014-75-C-0501
UNCLASSIFIED TI-08-77-39 NL

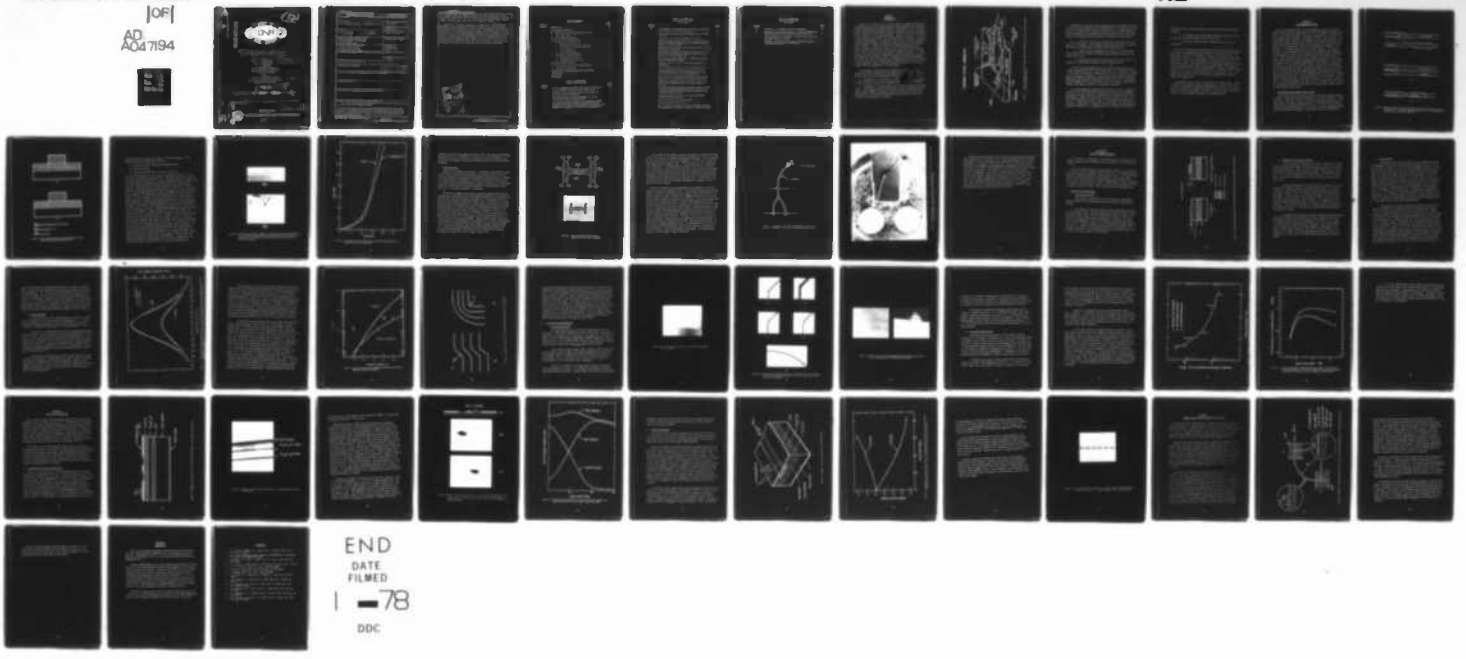

END
DATE FILMED
1-78
DDC

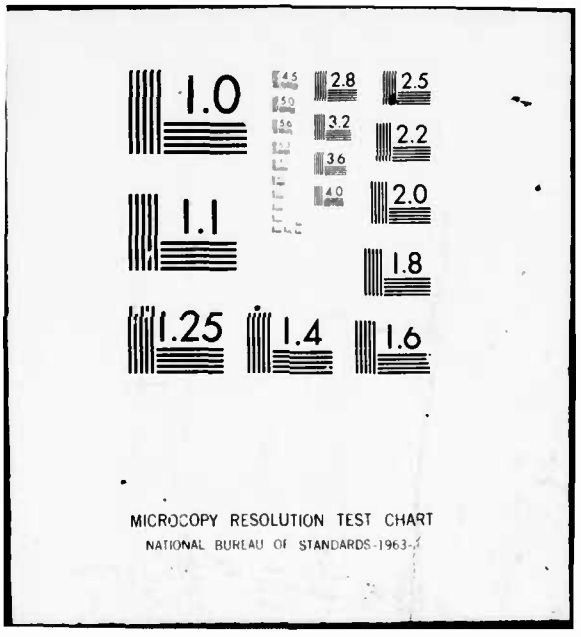
1.0
1.1
1.25
1.4
1.6
1.8
2.0
2.2
2.5
2.8
3.2
3.6
4.0
4.5
5.0
5.6
MICROCOPY RESOLUTION TEST CHART
NATIONAL BUREAU OF STANDARDS-1963-A

AD A047194

(12) B.S.

OFFICE OF NAVAL RESEARCH

(6) ACTIVE $Al_xGa_{(1-x)}As$ DEVICES FOR WAVEGUIDE CIRCUITS.

(10) A. R. Reisinger,
D. W. Bellavance,
J. C. Campbell
K. L. Lawley

Texas Instruments Incorporated
Central Research Laboratories
Dallas, Texas 75222

(14) TI-08-77-39

(15) Contract No. N00014-75-C-0501

ONR Contract Authority Identification
NR 009-015/10-24-74 427

DDC RECEIVED NOV 30 1977 A

(11) Oct[redacted]77 (12) 57p.

(9) Final Technical Report, [redacted] 3 Feb[redacted]75—31 May [redacted]77

Reproduction in whole or in part is permitted for any purpose of the United States Government.

DISTRIBUTION STATEMENT A
Approved for public release;
Distribution Unlimited

PREPARED FOR THE

OFFICE OF NAVAL RESEARCH ● 800 N. QUINCY ST. ● ARLINGTON ● VA ● 22217

DDC FILE COPY

403 833

UNCLASSIFIED

SECURITY CLASSIFICATION OF THIS PAGE (When Data Entered)

REPORT DOCUMENTATION PAGE

READ INSTRUCTIONS BEFORE COMPLETING FORM

1. REPORT NUMBER

2. GOVT ACCESSION NO.

3. RECIPIENT'S CATALOG NUMBER

4. TITLE (and Subtitle)
Active $Al_xGa_{1-x}As$ Devices for Waveguide Circuits

5. TYPE OF REPORT & PERIOD COVERED
Final Report

6. PERFORMING ORG. REPORT NUMBER
08-77-39

7. AUTHOR(s)
A. R. Reisinger
D. W. Bellavance
J. C. Campbell
K. L. Lawley

8. CONTRACT OR GRANT NUMBER(s)
N00014-75-C-0501

9. PERFORMING ORGANIZATION NAME AND ADDRESS
Texas Instruments Incorporated
13500 North Central Expressway
P. O. Box 5936
Dallas, Texas 75222

10. PROGRAM ELEMENT, PROJECT, TASK AREA & WORK UNIT NUMBERS

11. CONTROLLING OFFICE NAME AND ADDRESS
Office of Naval Research
800 North Quincy Street
Arlington, Virginia 22217

12. REPORT DATE
October 1977

13. NUMBER OF PAGES
51

14. MONITORING AGENCY NAME & ADDRESS (if different from Controlling Office)

15. SECURITY CLASS. (of this report)

15a. DECLASSIFICATION DOWNGRADING SCHEDULE

16. DISTRIBUTION STATEMENT (of this Report)

Reproduction in whole or in part is permitted for any purpose of the United States Government

DISTRIBUTION STATEMENT A
Approved for public release;
Distribution Unlimited

17. DISTRIBUTION STATEMENT (of the abstract entered in Block 20, if different from Report)

18. SUPPLEMENTARY NOTES

19. KEY WORDS (Continue on reverse side if necessary and identify by block number)

20. ABSTRACT (Continue on reverse side if necessary and identify by block number)

This report describes the accomplishments of the research program carried out under Contract No. N00014-75-C-0501.

Etched mesa double heterojunction GaAs/GaAlAs lasers were fabricated. Evanescent field coupling into an underlying (Ga/Al)As planar waveguide was achieved with 25% coupling efficiency. Selectively grown 1-bar mesa lasers were also successfully end-fire coupled into curved grown (Ga,Al)As waveguides with 35% efficiency.

DD FORM 1 JAN 73 1473 EDITION OF 1 NOV 65 IS OBSOLETE

UNCLASSIFIED

SECURITY CLASSIFICATION OF THIS PAGE (When Data Entered)

Next Page

Waveguide structures capable of channeling light around curves were investigated. Experiments indicate that, with current technology, an optimum radius of curvature is in the 1.27 to 2.54 mm (50 to 100 mil) range. Below 1.27 mm, radiation losses were found to increase very rapidly.

(Ga,Al)As active devices compatible with monolithic laser sources were developed. A new structure design, which includes a thin (~ 3000 Å) GaAs "cap," permits the fabrication of electroplated Pt Schottky barrier pads without significantly increasing the optical losses in the 8500 to 9000 Å wavelength range. Electrooptic directional coupler switches were made. A 17 dB extinction ratio in the coupled channel was measured at a reverse bias voltage of -25 V. Single-line, metal-gap modulators were also demonstrated with a modulation depth of 88% at a peak voltage of -25 V. These types of devices were successfully integrated with a 90° curved section of an ion-milled rib waveguide with a radius of curvature of 1.016 mm (40 mils). The major source of loss was the curve itself, which accounted for 17 dB of attenuation.

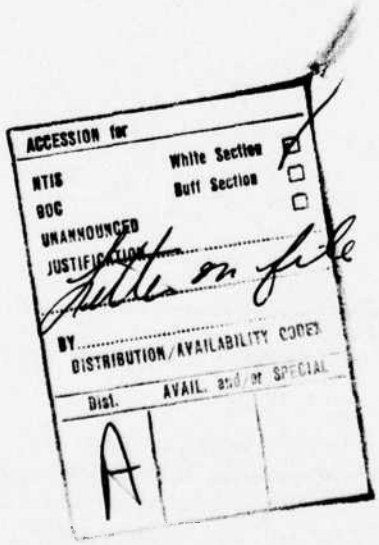

TABLE OF CONTENTS

LIST OF ILLUSTRATIONS

LIST OF ILLUSTRATIONS

(continued)

LIST OF ILLUSTRATIONS

(continued)

SECTION I
INTRODUCTION

The goal of the work carried out under Contract No. N00014-75-C-0501 was to develop modulators and switches compatible with monolithic lasers developed at Texas Instruments under separate programs. These parallel activities were aimed at advancing the technology required to fabricate a prototype integrated optical transmitter in the (Aℓ,Ga)As system. Figure 1 is an artist's schematic of the transmitter chip concept as envisioned at Texas Instruments. The device includes three components: (1) monolithic laser source, (2) passive waveguide circuits capable of channeling light around curves, and (3) active modulators and/or switches. The entire structure is fabricated monolithically on a single semiconductor substrate. Communication links using discrete semiconductor injection lasers and LEDs are becoming a commercial reality. In these systems, the light intensity is modulated by varying the diode drive current. The transmitter illustrated in Figure 1 represents an alternative approach in which the light source is operated cw while modulation and switching take place in the waveguide circuits. This approach permits optical multiplexing and signal processing independent of the light source.

The development of monolithic laser sources was carried out under a separate but parallel ONR contract, No. N00014-73-C-0252. Major accomplishments on that program which impacted this present program are as follows:

- Demonstration of laser action in a chemically etched, double heterojunction (DHJ) mesa structure with threshold current density of 2.4 kA/cm^2.
- Development of a new monolithic laser structure called an I-bar mesa laser. In these devices, which are selectively grown by liquid phase epitaxy (LPE), optical feedback is provided by naturally occurring vertical facets. The best devices were operated at 525 mA drive current with a pulsed, 300 K threshold current density of 7.5 kA/cm^2.

INTEGRATED OPTICAL TRANSMITTER

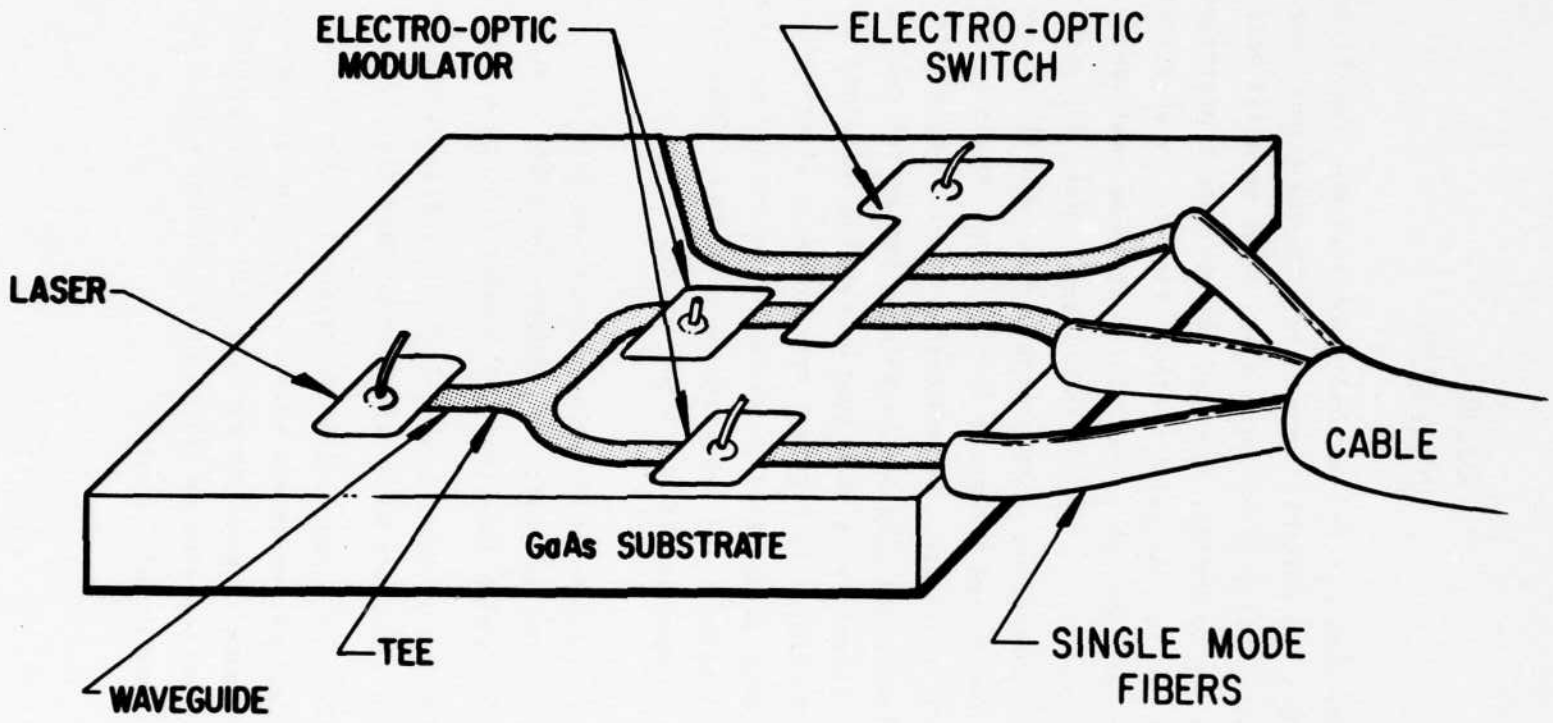

Figure 1 Artist's Schematic of a Monolithic GaAs IOC Transmitter with Its Outputs Coupled to a Fiber Optic Cable

Complementary to the laser effort mentioned above, the purpose of the contract was to develop (GaAℓ)As channel waveguides as well as modulators/switches. The choice of (GaAℓ)As was dictated by the requirement that these components must be transparent to the radiation emitted by the laser source. Three major problems were addressed during the course of this work, as discussed below.

(1) It is necessary to efficiently couple light from a monolithic laser source into a waveguide. Both evanescent-field coupling and end-fire coupling techniques were investigated, with the following accomplishments:

- Demonstration of evanescent-field coupling of an etched mesa laser structure into an underlying (GaAℓ)As planar waveguide with up to 25% coupling efficiency.

- Demonstration of end-fire coupling of an I-bar mesa laser into a selectively grown channel waveguide with up to 35% efficiency.

(2) Very little experimental data were available concerning the ability of channel waveguides to direct light around curves. As illustrated in Figure 1, such curves are required if integrated optical circuits (IOCs) are to achieve even a small degree of complexity. After optimizing the waveguide parameters, approximately 50% transmission was measured around a 90° curve in a dielectric stripline waveguide with a 3 mm (120 mil) radius of curvature. Radiation confinement deteriorates rapidly with increasingly severe curves.

(3) The development of (GaAℓ)As active devices was initially impeded by serious difficulties in fabricating Schottky barriers, apparently because of the formation of high resistivity interfacial layers between the metal and the semiconductor. These difficulties were overcome by growing structures with a very thin ($\sim$ 3000 Å) extra layer of GaAs. The thickness of the GaAs "cap" is too small to significantly increase the optical attenuation at the operating wavelength of 8500 Å, but its presence greatly facilitates the fabrication of

electrooptic pads. Using this technique, the following devices were demonstrated:

- Electrooptic directional-coupler/modulator switch with 17 dB extinction in the coupled channel at 25 V reverse bias.
- Single line modulator with ~ 90% modulation depth at 25 V reverse bias.

Because of the greater facet perfection of selectively grown devices, the I-bar laser can be expected to be more amenable to cw operation than etched mesa lasers. Emphasis was consequently placed on the former structure. As discussed in Section II, it is necessary to channel the output of these lasers around a 45° bend to take full advantage of the electrooptic effect in the GaAs/(GaAℓ)As system. The feasibility of this concept was demonstrated by combining an ion-beam etched, curved channel waveguide [radius of curvature of 1.016 mm (40 mils)] with a single-line modulator. A modulation depth of 30% was measured in this device with an attenuation of 17 dB around the curve. Integration of an I-bar laser with a curved channel waveguide and a modulator remains to be demonstrated.

The remainder of this report is divided into four major sections. Section II addresses the problem of laser-waveguide coupling. Section III is a discussion of curved channel waveguides. Modulators and switches in the (GaAℓ)As materials system are the subject of Section IV. Section V describes the integration of a curved channel waveguide with a GaAℓAs modulator.

SECTION II
LASER-WAVEGUIDE COUPLING

One of the key problem areas in the development of IOCs is efficiently coupling from a monolithic laser source to a thin-film channel waveguide. This is also an area that has received relatlvely llttle attention. The most commonly proposed coupling schemes, illustrated in Figure 2, are evanescent field coupling and end-fire coupling. The evanescent field coupling technique relies on radiation leakage from the active junction region of the laser diode to an underlying passive waveguide. There are two approaches to evanescent field coupling: (1) resonant coupling, and (2) "strong" coupling. For resonant coupling, or weak evanescent field coupling, the radiation transfer mechanism is the same as that taking place in waveguide directional couplers [see Figure 2(a)]. Efficient coupling requires that the phase velocities of the laser cavity and the underlying passive waveguide be closely matched. The stringent requirements that this coupllng scheme imposes on the growth of the multilayer structures limit its use for practical devices. For the case of strong evanescent field coupling, the active and passive waveguides are in close proximity and are strongly coupled without phase coherence. The evanescent field from the active waveguide is used to excite waveguide modes of the underlying passive waveguide [see Figure 2(b)]. We have emphasized this latter approach. In the end-fire coupling technique, illustrated in Figure 2(c), the laser is coplanar with the end of the waveguide. The dlfficulty of this method is the criticality of the alignment between the active layer of the laser and the waveguide layer to minimize the insertion loss.

A. Etched Mesa Double-Heterostructure Lasers

We have fabricated two structures having active lasers coupled to passive waveguides. These laser waveguide devlces are illustrated in Figure 3. Figure 3(a) shows a five-layer structure in which the n-type (Aℓ,Ga)As heterobarrier also serves as the passive waveguiding layer. A variation of this structure [Figure 3(b)] has an addltional thln, low index, slxth layer sandwiched between the active and passive waveguldes. Both the structures are fabricated by

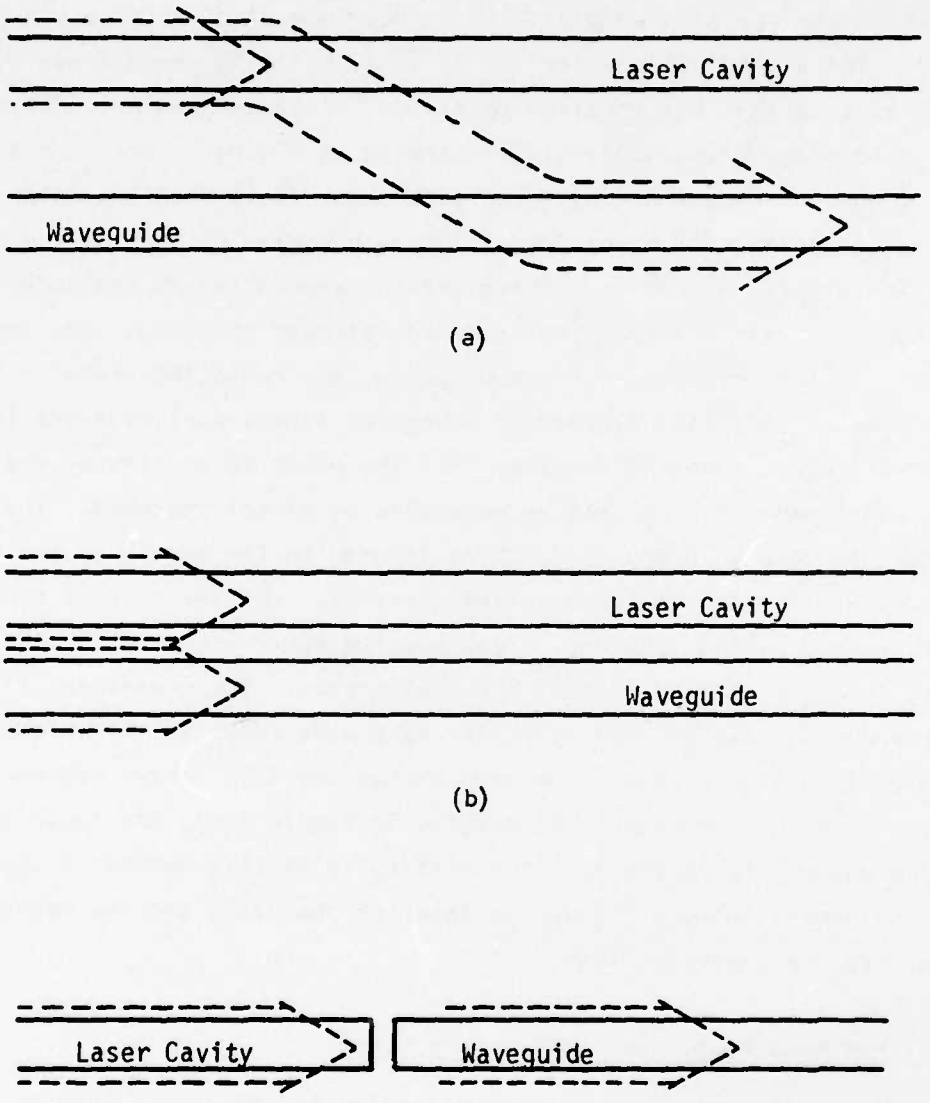

Figure 2 Schematic Diagram Illustrating Coupling Between the Laser Cavity and the Waveguide. (a) Weak evanescent coupling, (b) strong evanescent coupling, and (c) end-fire coupling.

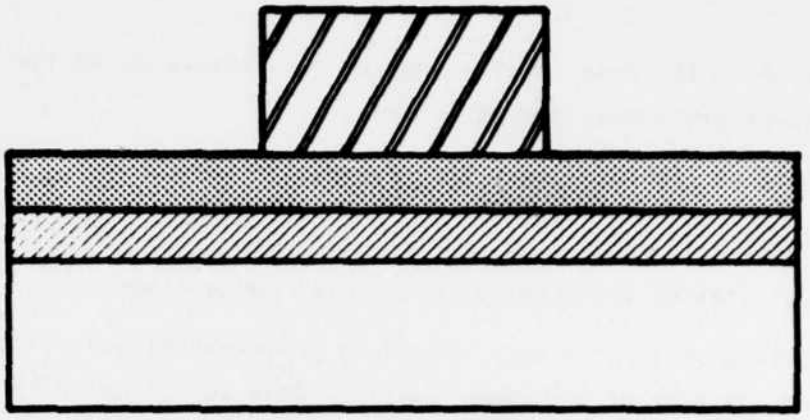

(a)

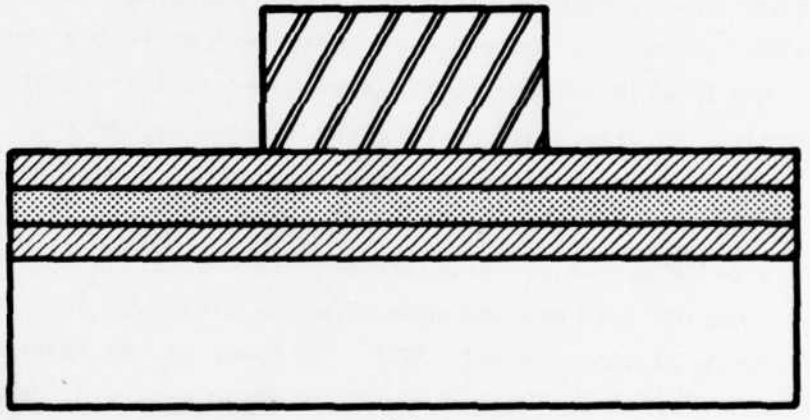

(b)

Double Heterostructure Mesa Laser

$n\text{-}Ga_{1-x}Al_xAs$ $(x < y)$

$n\text{-}Ga_{1-y}Al_yAs$

Figure 3 Two Laser-Waveguide Structures Showing (a) Strong and (b) Weak Coupling Configurations

selectively etching the laser cavity down to the passive waveguide. The fabrication steps are summarized as follows:

(1) Growth of the multilayer laser/waveguide structure

(2) Masking with SiO_2

(3) Metallization and mounting electrical contacting.

After etching through the top four layers, a preferential GaAs etch[1] is used to "square up" the ends of the laser cavity. This additional etch can make the difference between a device that will lase and one that will not. To date, the best room temperature threshold current densities that we have achieved for five- and six-layer devices are 3.6 and 2.4 kA/cm^2, respectively. Figure 4 shows (a) a cleaved and stained cross-sectional view of a five-layer structure and (b) a device under operation with laser light emerging from the end of the planar waveguide. A primary concern with these devices is the coupling efficiency, i.e., the fraction of the total laser power that is coupled into the passive waveguide. To determine the coupling efficiency, we first measure the total power from the laser and the waveguide with a calibrated PIN photodiode. The power from the laser is then blocked off so that only the light emerging from the waveguide is detected. From these measurements the coupling efficiency can easily be computed. In devices made from the six-layer structure the coupling efficiency is approximately 10%. The power in the laser and the waveguide as a function of the drive current is shown in Figure 5. The power in the waveguide increases superlinearly for currents above the lasing threshold, and the onset of lasing is the same for both curves. This confirms that laser emission as well as spontaneous radiation is coupled into the waveguide. In the five-layer devices measured coupling efficiencies have been as high as approximately 24% and as low as approximately 1%. As one might expect, the devices having higher coupling efficiencies also have higher lasing thresholds because the coupling is an additional loss mechanism. The additional loss caused by coupling into the waveguide could be offset by reducing the light lost from the ends of the laser cavity. This could be accomplished by

(a)

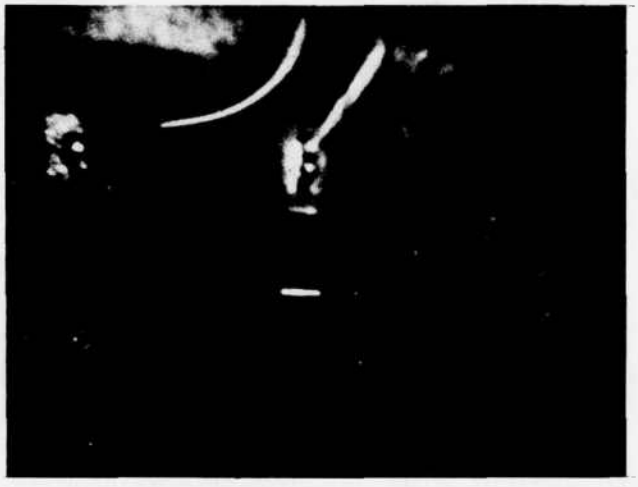

(b)

Figure 4 (a) Photomicrograph (~ 1000X) of a Cleaved and Stained Cross Section of a Five-Layer Etched DHJ Mesa Laser-Waveguide; (b) Top View of Structure in (a) Showing Light Emission at the Edge of the Chip (From the Waveguide)

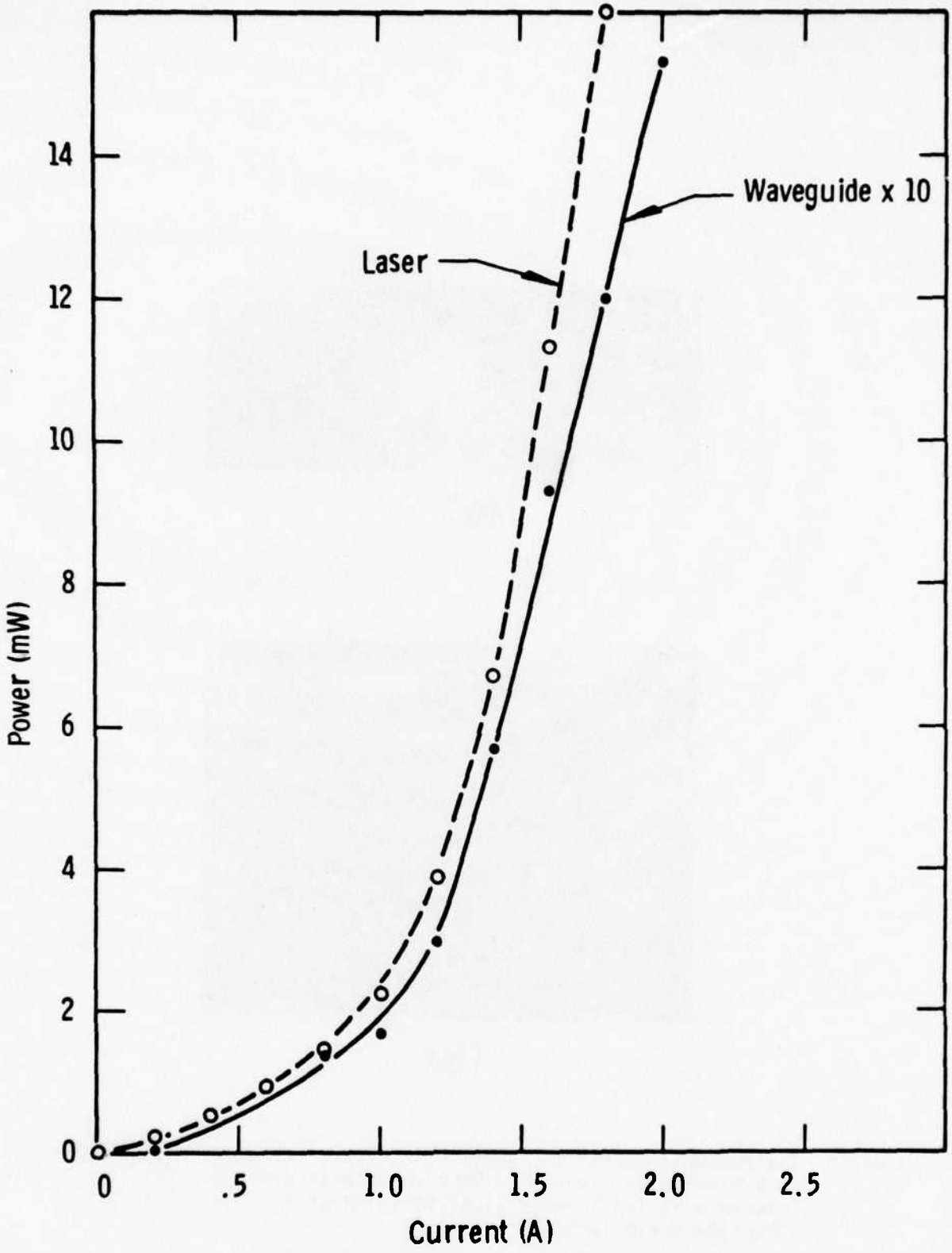

Figure 5 Power Output of an Etched Laser and Underlying Waveguide as a Function of Laser Drive Current

evaporating mirrors on the ends of the laser cavity. The coupling efficiencies quoted above refer to the amount of light fed into a planar waveguide. No attempt has been made yet to couple an etched mesa laser into a narrow channel waveguide.

B. I-Bar Mesa Laser

Although the threshold current densities achieved in etched double heterostructure mesa lasers are most encouraging, these devices suffer from the inherent drawback that no presently known chemical etching procedure is capable of producing smooth, vertical walls in multilayer heterojunction structures. The problem, which can be appreciated by inspection of Figure 4(a), undoubtedly imposes limitations on the ultimate performance of these monolithic lasers, particularly with regard to possible cw operation.

An alternative method of fabrication of monolithic laser sources was developed under separate ONR contract, No. N00014-73-C-0288.[2] Briefly summarized, the technique is based on selective LPE growth of III-V compounds along preferred crystallographic orientations through silicon nitride masks. For {100} GaAs substrates, vertical facets with a high degree of perfection can be grown along the edges of stripes aligned parallel to the [010] and [001] directions. By combining three such stripes in the manner illustrated in Figure 6, the so-called I-bar mesa laser structure is obtained. In this new structure the central member serves as the laser cavity, while the perpendicular facets at either end provide the optical feedback. The best device tested to date had a room-temperature, pulsed threshold current density of 7.5 kA/cm^2, corresponding to a drive current of 525 mA.[2] The active layer thickness was approximately 1 μm. External differential quantum efficiencies have been measured with a calibrated PIN photodiode,[3] and values as high as 15% have been observed. Additional technical details can be found in Reference 2.

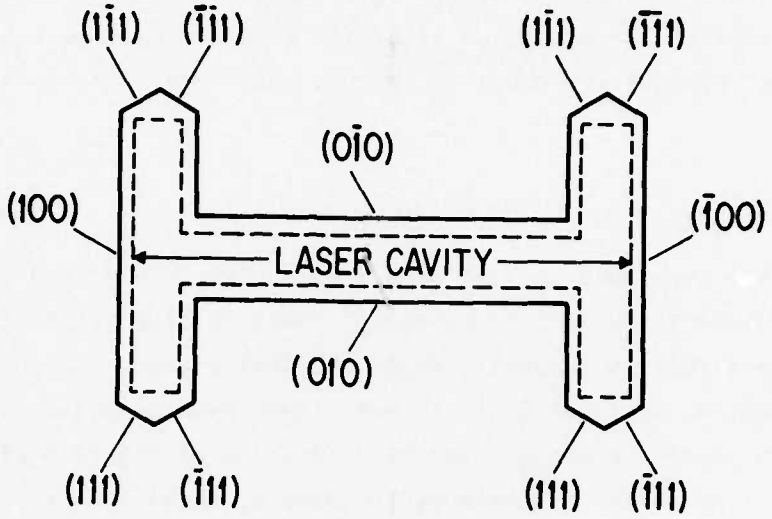

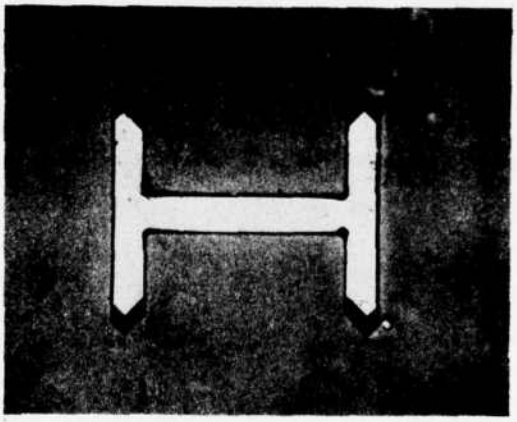

Figure 6 I-Bar Mesa Showing Mask Opening (dashed line) and Facet Formation

In the context of the present contract, the problem of coupling the output of these I-bar lasers into channel waveguides was addressed. It was recognized that the light exiting an I-bar laser propagates in a direction for which the electro-optic effect is exactly zero. If an I-bar laser is to be integrated with a modulator, it is thus necessary to deflect the light by an angle of ± 45° with respect to the direction of the laser cavity to take full advantage of the electro-optic properties of the material. Straight and curved channel waveguides can be grown with the same selective LPE technique discussed above in connection with the fabrication of I-bar mesa lasers. The properties and characteristics of these curved channel waveguides are discussed in detail in Section III of this report.

Selective LPE mesa lasers and waveguides can be combined in a two-step process to produce an integrated circuit. This has been accomplished and marks a major milestone in the progress of this program. The overall design of the device as shown in Figure 7 consists of two separate masks, one for the waveguide structure and one for the mesa laser structure. In the first growth step the three-layer waveguide structure is grown in the waveguide pattern only. The mesa laser area in this step is covered by the silicon nitride mask. After the first growth step, the silicon nitride mask is stripped and the entire substrate, including the grown waveguide, is covered with fresh silicon nitride. The laser pattern is then opened in the mask and the DH I-bar mesa laser is grown in the second LPE growth step. The laser in this circuit is end-fired into the waveguide. Ohmic contact to the back of the unthinned substrate is made by alloying electroplated Ni-Au at 300°C. The p-type contact on the top of the mesa is made by evaporating Cr-Au. A wide bonding pad at the side of the mesa permits off-mesa bonding. The final test device is cleaved along line A of Figure 7 to give single-channel light output. A finished device mounted on a TO-46 header is shown in Figure 8.

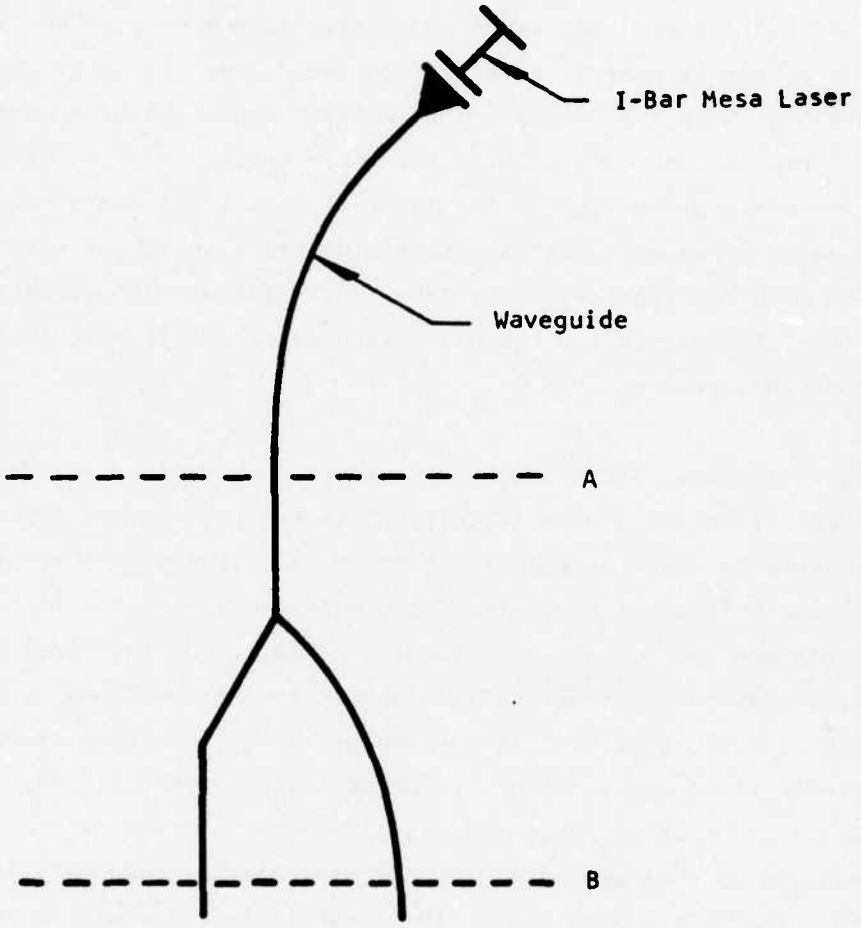

Figure 7 Integrated I-Bar Mesa Laser-Waveguide Structure

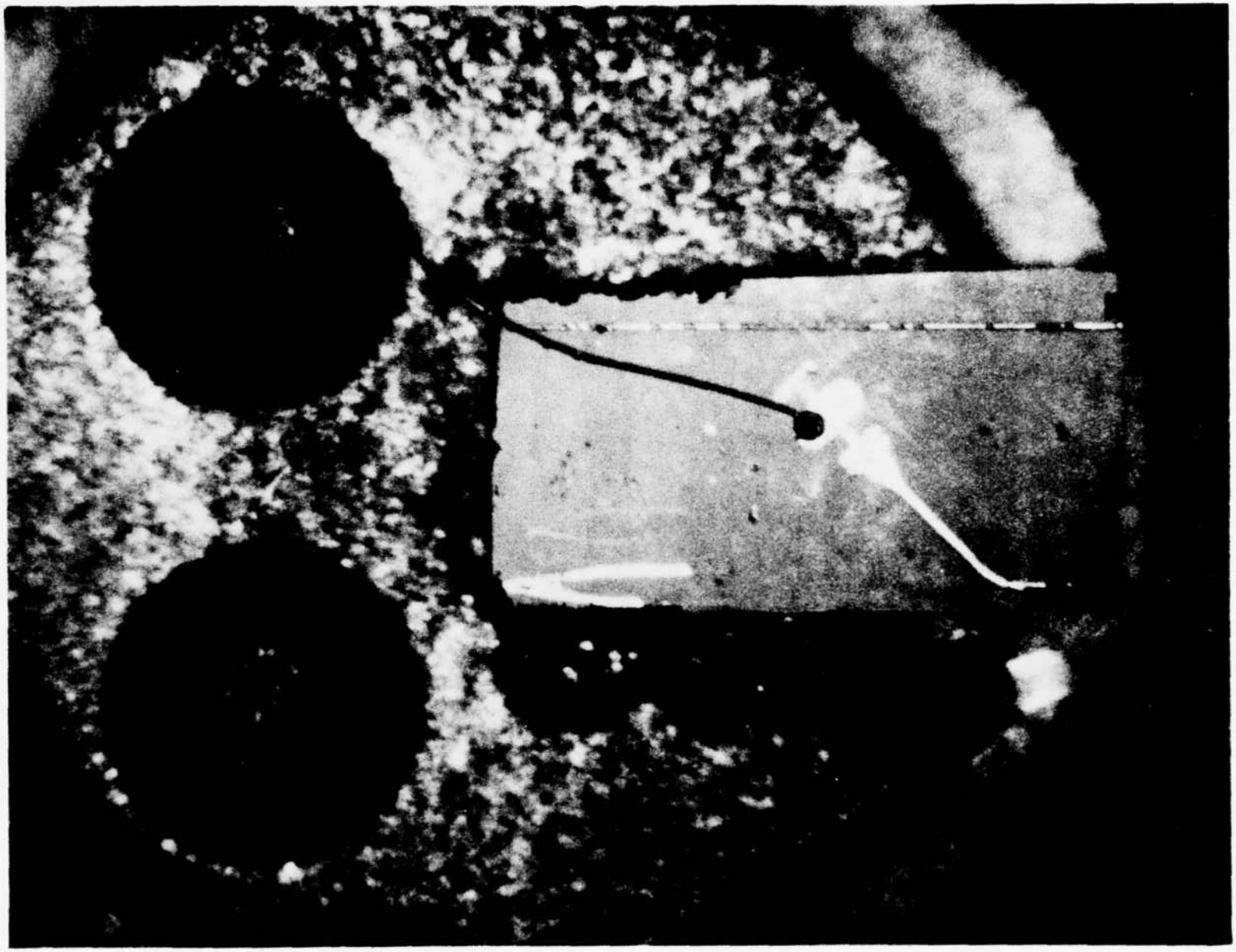

Figure 8 Photomicrograph (~ 10X) of the First Integrated Optical Circuit with an I-Bar Mesa and Curved Channel Waveguide Mounted on a TO-46 Header

Integrated 1-bar mesa lasers end-flring into curved waveguides were tested. These devices had active regions of 1.5 μm and correspondingly high thresholds of 40 kA/cm^2. The as-grown waveguides are three-layer structures with nominal compositions of $Ga_{0.8}Al_{0.2}As$ - $Ga_{0.85}Al_{0.15}As$ - $Ga_{0.8}Al_{0.2}As$ with the central layer about 4.0 μm thick. Laser radiation from the 1-bar was end-fired-coupled to the curved waveguide. Its radius of curvature was a severe 0.254 mm (10 mils). Measurements of the light transmitted through the waveguide and from the laser showed a transmission of about 35% of the laser output. The output was narrowband, suggesting that a selection of laser modes is taking place. The transmission figure was based on the power in the narrowband laser output, not on the total emission power spectrum of the laser. This unexpected selectivity is not understood at this time.

SECTION III
(Aℓ,Ga)As CHANNEL WAVEGUIDES

This section is a discussion of the characteristics of (Aℓ,Ga)As passive channel waveguides that are needed to optically connect any two points on an IOC chip.

Two fabrication techniques were investigated. The first is an extension of a method previously developed in GaAs structures.[4] It is based on chemical etching of waveguiding patterns in planar epitaxial layers. The second is the selective LPE growth technique briefly described in the previous section. Three important characteristics of channel waveguides are (1) their attenuation in straight sections, (2) their ability to confine light, and (3) their ability to channel light around a bend. These characteristics are discussed below.

A. Etched Stripline Waveguides

1. Waveguide Fabrication

Both dielectric striplines and rib striplines were investigated. Schematic drawings of these waveguide structures are shown in Figures 9(a) and 9(b).

The as-grown structure for dielectric stripline waveguides consists of three (Aℓ,Ga)As layers. The middle waveguiding layer has a lower Aℓ concentration and hence a higher refractive index than the other two layers. The stripline is formed by selectively etching back the top layer. The typical width of these waveguides is 10 μm; the thickness of the waveguiding layer d is 1.5 to 2.5 μm; and the difference in the Aℓ concentration between layers Δx is 0.05 to 0.1. However, devices having d as small as 0.5 μm and $\Delta x \sim 0.3$ have been fabricated. The rib waveguides have only two (Aℓ,Ga)As layers, and a ridge is selectively etched into the top layer.

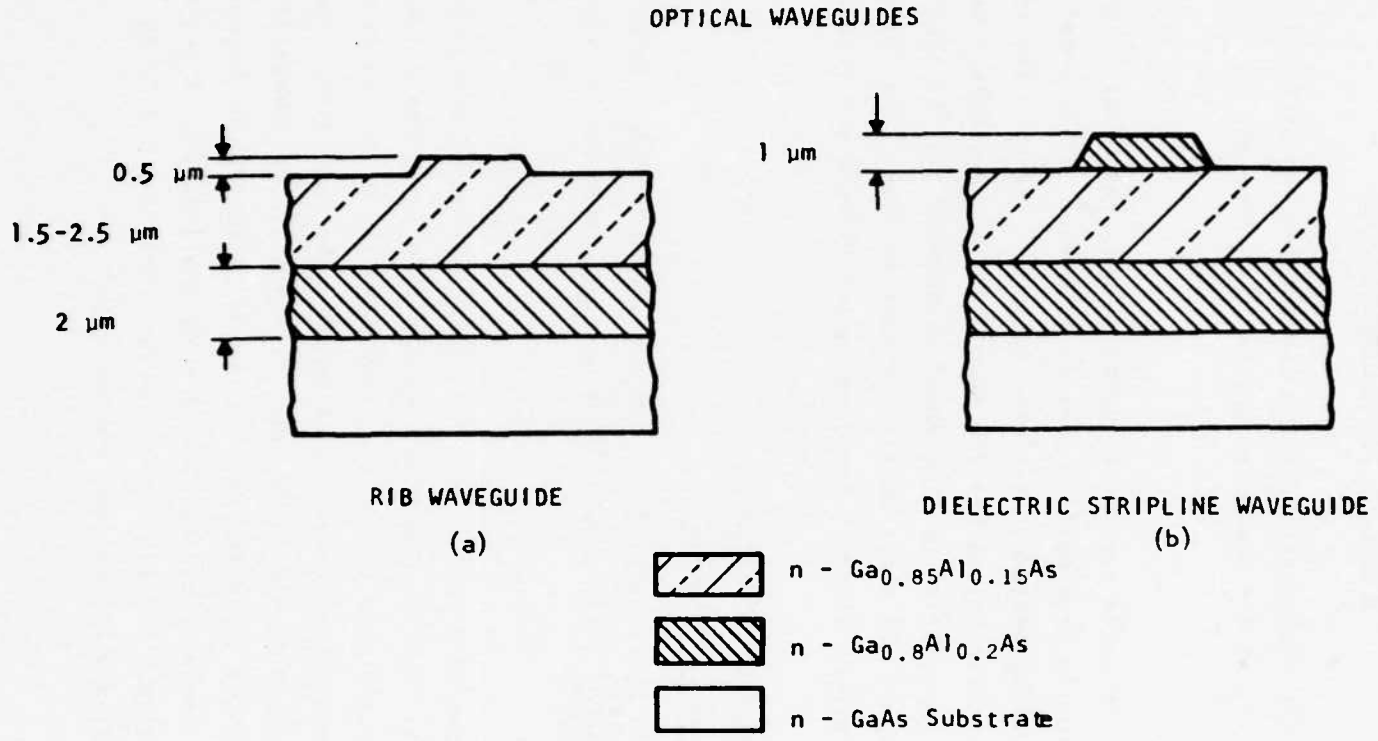

Figure 9 Schematic Drawings of (a) Rib and (b) Dielectric Stripline Waveguides in (Ga,Aℓ)As

2. Attenuation in Straight Waveguides

A general observation made during this work is that epitaxial layers grown by LPE often have rougher interfaces and larger variations in thickness than those grown by VPE. This can result in higher attenuation in the waveguides due to scattering losses and mode conversion. These problems are not as critical for small devices such as injection lasers, but they can become severe limitations for waveguide circuits that are typically several millimeters long.

In addition to mode conversion, uneven epitaxial layers give rise to a more severe problem in regard to the fabrication of dielectric stripline waveguides. These devices require selective etching through the top layer to the waveguiding layer. This is a crucial step with small tolerances on the etch depth. If the top layer is not etched far enough, little or no light confinement will be observed. On the other hand, it is important to avoid etching through the waveguiding layer, since this will produce a very lossy waveguide. If the top layer thickness varies significantly, a waveguide that has been etched correctly in one region will become unacceptable at another point along its length.

The attenuation coefficient of several (Aℓ,Ga)As waveguides has been determined by measuring the transmission of several lengths of each sample. The losses in dielectric stripline waveguides are typically in the range of 7 to 9 dB/cm, with 5.3 dB/cm being the lowest value. This can be compared with an average of 4 dB/cm for VPE GaAs waveguides. Rib waveguides have slightly higher losses, typically in the range of 10 to 12 dB/cm, with the lowest value 7.2 dB/cm. All these measurements were made at 1.06 μm. The losses will be slightly higher for laser diode sources emitting at 8500 to 9000 Å.

3. Field Profiles

A knowledge of the energy distribution of the propagating radiation in a waveguide is required for proper design of waveguide circuits. Of particular interest for optical striplines is the exponential decay of the fields away from the patterned strip. For a directional coupler the decay length ζ should be long to insure good communication between channels. On the other hand, the minimum bend radius of a stripline is proportional to the third power of the decay length ζ.[5] Therefore, for circuits requiring curved waveguides, the decay length should be kept as small as possible. Two methods of calculating the field profiles of stripline waveguides have been reported. The first method[6,7] assumes a pseudo-index discontinuity in the waveguiding layer at the edges of the stripe overlay. A second approach developed by Butler, et al.,[8] uses spatial interference of plane waves to achieve optical confinement in the slab region underneath the strip. We have found that this theory, referred to as the SPW method, yields more consistent agreement with our experimental data than the pseudo-index approach.

The apparatus for measuring the energy distribution uses a Nd:YAG laser beam focused onto the cleaved edge of the waveguide (spot diameter $\simeq$ 2 μm). The input laser beam is polarized so as to excite only TE modes. A magnified image of the near-field intensity pattern at the waveguide output is focused on a 160 μm diameter pinhole that has been affixed to a PIN photodiode and mounted on a translation stage that is driven with a small electric motor. The optical signal is detected with a lock-in amplifier and plotted on a chart recorder. Using this apparatus the pinhole can be scanned parallel to the dielectric interfaces (i.e., in the x direction) at any point y in the waveguiding layer between the patterned strip and the substrate. This permits a two-dimensional mapping of the modal pattern of the waveguide. The experimental resolution of these modal patterns is limited by the finite size of the pinhole and the sensitivity of the micrometer on the translation stage. We estimate the resolution to be 0.27 μm in both the x and y directions. In

Figure 10 the dashed curve shows two scans along the x direction of the waveguide. The upper curve was obtained by locating the field peak at the center of the waveguide ($x = 0$). The lower curve was obtained at an arbitrary value of y below the peak. The solid curves in Figure 10 show field plots calculated by the SPW method. The upper curve was calculated by finding the peak field at $x = 0$. The lower curve was made at an appropriate y location to best match the experimental field. Although the curves in this figure illustrates good agreement between theory and experiment, in general the calculated curves differ by less than 10% from those obtained by scanning the output intensity.

4. Curved Waveguides

To determine the ability of (Aℓ,Ga)As optical striplines to channel light around bends, we first investigated tilted waveguides, i.e., straight sections intersecting at an angle. This was done to provide "worst-case" information. Photomasks were designed with tilt angles between 0.1° and 1.1°.

Two sets of tilted (Aℓ,Ga)As optical stripline waveguides were fabricated and tested. One set of dielectric striplines has waveguides 6.6 μm wide and 2.1 μm thick and has a refractive index step of approximately 0.02. The second set of rib waveguides is 8.7 μm wide, 2.5 μm thick, and has a refractive index step of about 0.02. For both sets of waveguides the transmitted power decreases by a factor of two when the tilt angle is in the range $0.7° \leq \zeta \leq 1°$. Using the pseudo-index approach, we calculate that maximum bend angle should be in the range 0.8 to 1.2°.

Abrupt angular discontinuities are clearly unsatisfactory from the standpoint of attenuation. Continuous bends are therefore required to change the direction of propagation of an optical guided wave. However, curved waveguides also exhibit intrinsic radiation losses,[5] and experimental data are needed to determine how the radius of curvature affects bending losses in a specific device configuration.

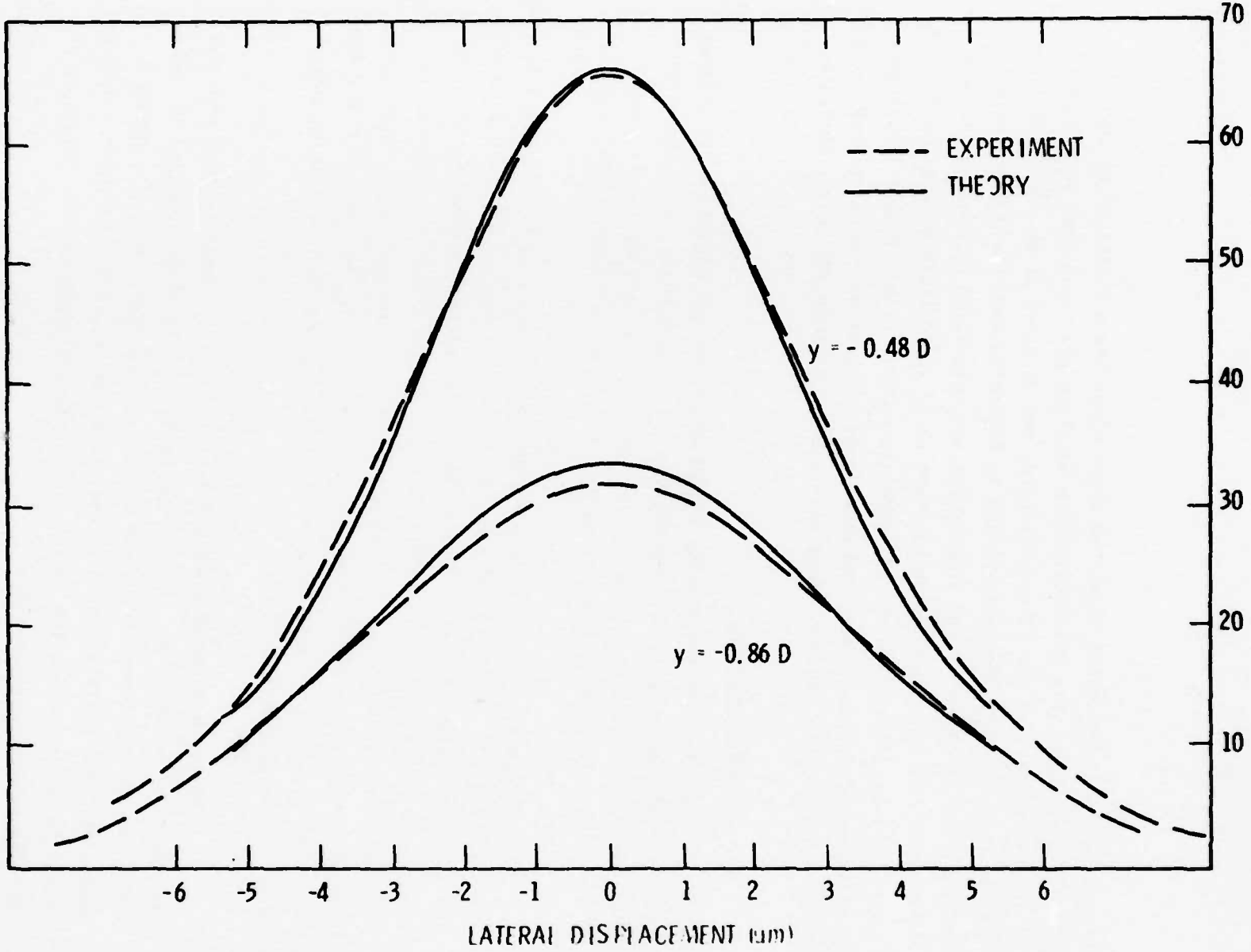

Figure 10 Experimental (Dashed) and Theoretical (Solid) Intensity Distribution of Light as a Function of Position in a Dielectric Stripline Waveguide. (See Reference 8 for definition of parameters y and D.)

The optimum optical stripline structure for channeling light around a bend is one that gives maximum confinement under the strip and minimizes the characteristic decay length ξ away from the strip. Since the minimum bend radius R_{min} is proportional to ξ^3, ξ was calculated as a function of three waveguide parameters: (1) the width of the strip, (2) the magnitude of the refractive index steps between layers, and (3) the thickness of the waveguiding layer. We find that ξ is relatively insensitive to changes in the waveguide width and refractive index discontinuities, but varies sharply with the thickness of the waveguiding layer. Figure 11 shows the minimum radius of curvature as a function of the waveguide thickness calculated by both the pseudo-index method and the SPW method for various waveguide thicknesses. Note that the pseudo-index method predicts smaller values of R_{min} than the SPW method.

To measure the light channeled around a curved section of waveguide, several sets of photomasks, shown in Figure 12, were designed. Two sets [Figure 12(a)] are S-like and permit observation of the guided light at the opposite end to the waveguide input. On one photomask the net displacement between the straight sections is 0.127 mm (0.005 inch), and the radii of curvature of the connecting arcs are 0, 0.635, 1.27, and 2.54 mm (0, 25, 50, and 100 mils). The second S-like curves have radii of curvature of 1.016, 2.54, 5.08, and 10.16 mm (40, 100, 200, and 400 mils). The third set of waveguides [Figure 12(b)] has full 90° bends with radii of curvature of 11.176, 9.144, 7.112, 5.08, 3.048, and 1.016 mm (440, 360, 280, 200, 120, and 40 mils). Initial investigations involved waveguides having a waveguiding layer 1.7 to 4.0 μm thick. In all cases the minimum radius of curvature was found to be greater than 10 mm (400 mils). We estimate that only a few tenths of a percent of the incident light was channeled around the bend. This agrees with the SPW calculations and contradicts the pseudo-index calculations. Since our calculations indicate that waveguides with thin waveguiding layers are better suited to channeling light around curves, we have grown and fabricated waveguides with 0.5 μm thick waveguide layers. These waveguides have exhibited

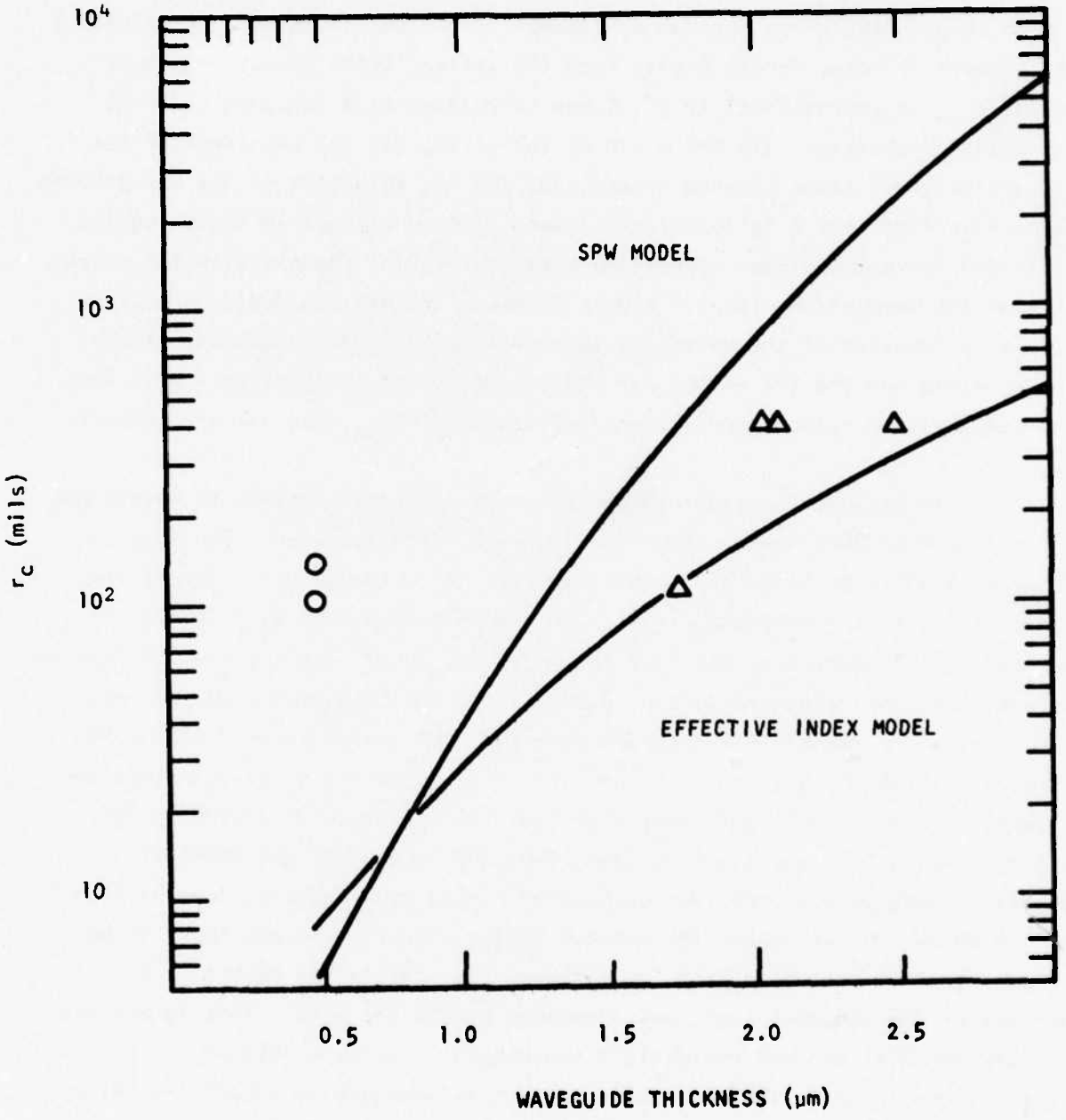

Figure 11 R_{min} as a Function of Waveguide Thickness Calculated by SPW and Pseudo-Index Methods

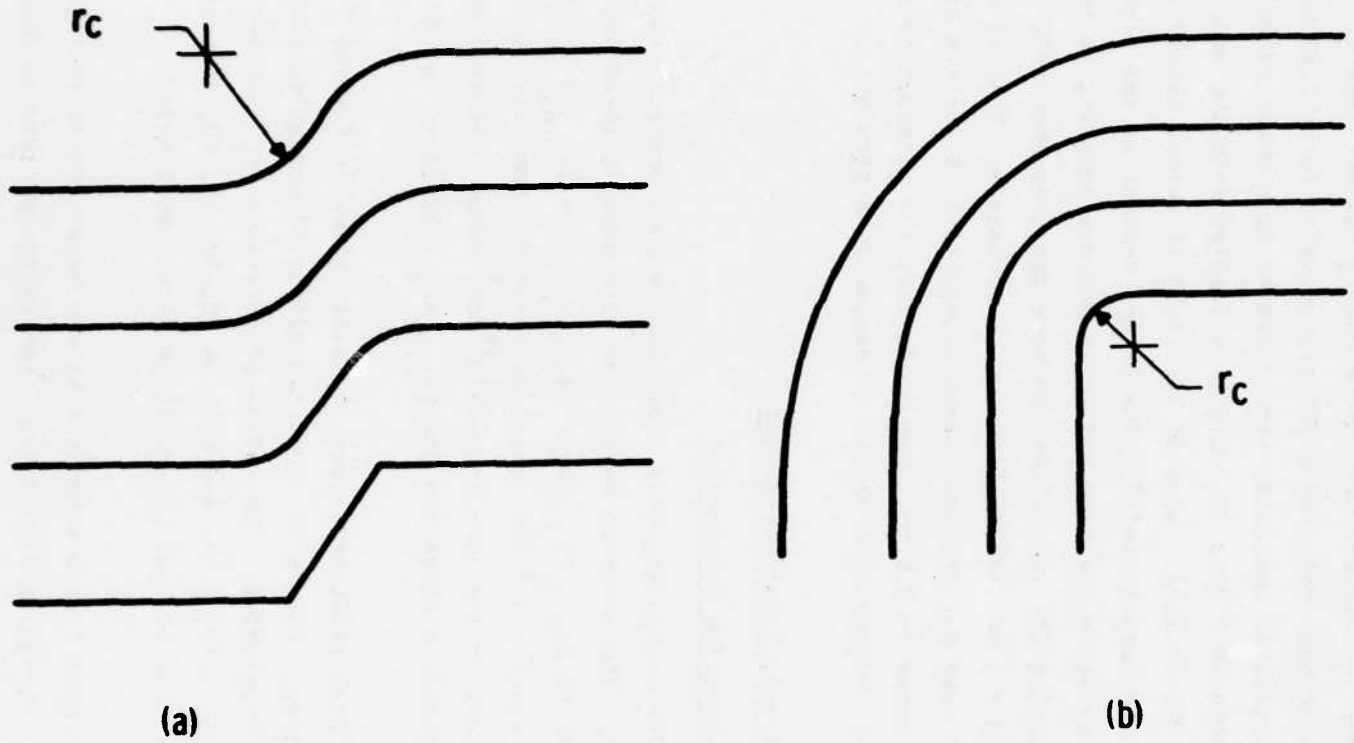

Figure 12 Schematic Drawing of Various Bend Configurations for Waveguides

a significant improvement over those having thicker layers. Using the S-like waveguides, we have measured a 38% transmission for a 2.54 mm radius of curvature. With similar waveguide structures we have observed guiding around 90° bends as shown in Figure 13. Light is coupled into the waveguide at the lower portion of the picture. Some of the light is guided around the bend and can be seen at the output (left). The bright regions at top right result from radiation losses in the bend and in incomplete coupling at the waveguide input. After correcting for the latter, we have measured about 50% transmission in a curve having a 3 mm (120 mil) radius of curvature. This is a significant improvement over our original thick waveguides. Given the propagation length around the curve ($\sim$ 0.5 cm), one finds that the attenuation coefficient is about 6 dB/cm higher than if the waveguide were straight.

B. Selectively Grown Waveguides

1. Waveguide Fabrication

The waveguides were grown by the same process used for the I-bar mesa lasers. The as-grown waveguides were usually three-layer structures with compositions of $Ga_{0.85}Al_{0.15}As$ - $Ga_{0.9}Al_{0.1}As$ - $Ga_{0.85}Al_{0.15}As$. Each layer is about 2 μm thick. All the layers were n-type, nominally undoped, with carrier concentrations in the low- to mid-$10^{16}/cm^3$ range. Several two-layer structures were also grown in which the top $Ga_{0.85}Al_{0.15}As$ layer was omitted.

Three different types of masks, shown in Figures 7 and 12, were used for this study. Figure 12 shows two different waveguide patterns used only for waveguide studies. The radius of curvature (r_c) was set at values of 0, 0.254, 0.635, 1.27, 2.54, and 6.35 mm (0, 10, 25, 50, 100, and 250 mils). Stripe widths of both 10 μm and 25 μm were investigated.

Figure 7 is a schematic of the mask used to fabricate integrated I-bar laser/waveguide structures. For waveguide test purposes, this pattern was cleaved along lines A and B. The two "legs" of the remaining structure had

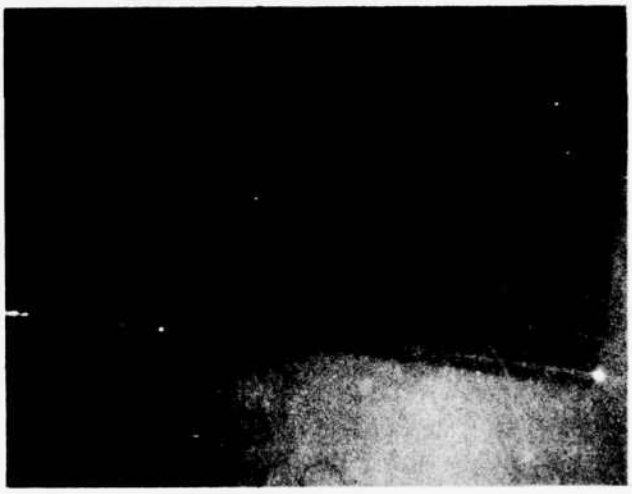

Figure 13 Light Propagating Through a Thin 90° Bend Waveguide.
R_c = 120 mils.

(a)

(b)

(c)

(d)

(e)

Figure 14 As-Grown Waveguides with Radii of Curvature (a) 0, (b) 0.254 mm (10 mils), (c) 0.635 mm (25 mils), (d) 1.27 mm (50 mils, and (e) 6.35 mm (250 mils)

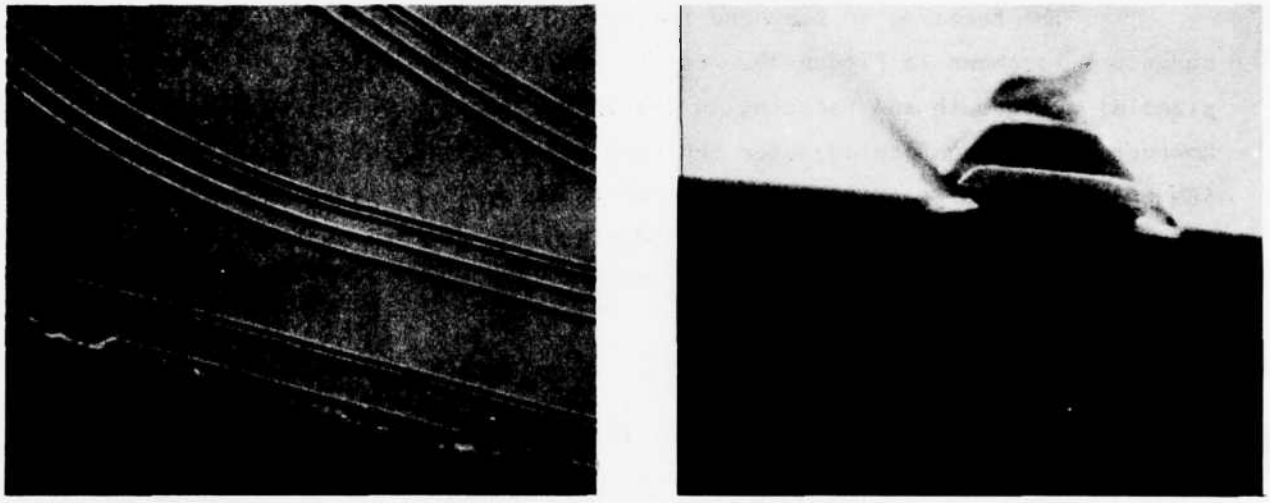

Figure 15 SEM of Selective LPE Waveguides Showing Growth Around a Bend and a Cross Section of a Three-Layer Waveguide

r_c values of 0 (9° angle of incidence) and 1.27 mm (50 mils). Only 25 μm stripe widths were used in this pattern. The unusual structural features of this pattern include the Y divider in the cleaved portion of the structure and the "funnel" at the top of the guide for collecting light from the laser.

The faceting in the bend for waveguides with different radii of curvature is shown in Figure 14. For $r_c \leq 0.254$ mm (10 mils), there is substantial overgrowth and faceting in the bend. For $r_c \geq 0.635$ mm (25 mils), however, smooth nonfaceted outer surfaces can be obtained. Figure 15 shows SEM photographs of sets of four 10 μm wide, three-layer waveguides with r_c = 1.27 mm (50 mils) and 2.54 mm (100 mils) and a cross section of a three-layer waveguide.

2. Waveguide Characteristics

Light guiding has been observed for all waveguide structures, including r_c = 0 (9° angle of incidence) with 2 to 3 μm thick waveguide layers. As expected from the larger index discontinuity, the losses in straight-line sections are higher for the selectively grown waveguides (9 to 18 dB/dm) than for the etched LPE (Aℓ,Ga)As dielectric stripline waveguides. The loss values are also enhanced by materials inhomogeneities and defects in the long guide sections required to make these measurements. Improvements in the materials growth process would be expected to lessen the contribution from this area.

As expected, the trend is toward increasing loss with decreasing radius of curvature. Rapid degradation occurs for $r_c < 1.27$ mm (50 mils) and places a lower limit on the range of interest for practical circuit design.

Similar behavior was observed for the waveguide section of Figure 7 where the relative outputs of the two "legs" was $r_c(1.27\ mm)/r_c(0) \sim 12$. Attenuation coefficients are plotted against radius of curvature as open circles in Figure 16. The graph of Figure 16 also contains an open triangle which represents a dielectric stripline waveguide illustrated in Figure 13, as well as an open square data point corresponding to an ion-milled rib waveguide which will be discussed in Section V.

Figure 16 is a summary of the best results achieved to data at Texas Instruments. It shows that the various techniques we have investigated appear comparable, so far, in terms of ability to channel light around a curve. While the data contained in Figure 16 should not be construed as the ultimate limit achievable, these values do represent the current state of the art in (Aℓ,Ga)As curved channel waveguides.

For very sharp curves, the radiation losses are dominant. On the other hand, for gentle curves, the propagation distance required to achieve a given angular deviation can be quite long, and the scattering losses take over. Consequently, there is an optimum radius of curvature that is the best compromise between the two loss mechanisms. On the basis of the "average" curve drawn in Figure 16, the total attenuation per unit angle of deflection can be calculated as a function of radius of curvature. The results are shown in Figure 17, where curves A and B correspond to a straight-line attenuation of 10 dB/cm and 20 dB/cm, respectively. In the latter case, the optimum radius of curvature r_c is between 1.3 and 2 mm (50 and 80 mils) with a minimum attenuation of 6.5 dB/rad. Thus, for a 90° bend the amount of light would be attenuated by about 10 dB. For a straight-line attenuation of 10 dB/cm, the optimum r_c is between 1.5 and 2.8 mm (60 and 110 mils) with a minimum attenuation of 4.6 dB/rad.

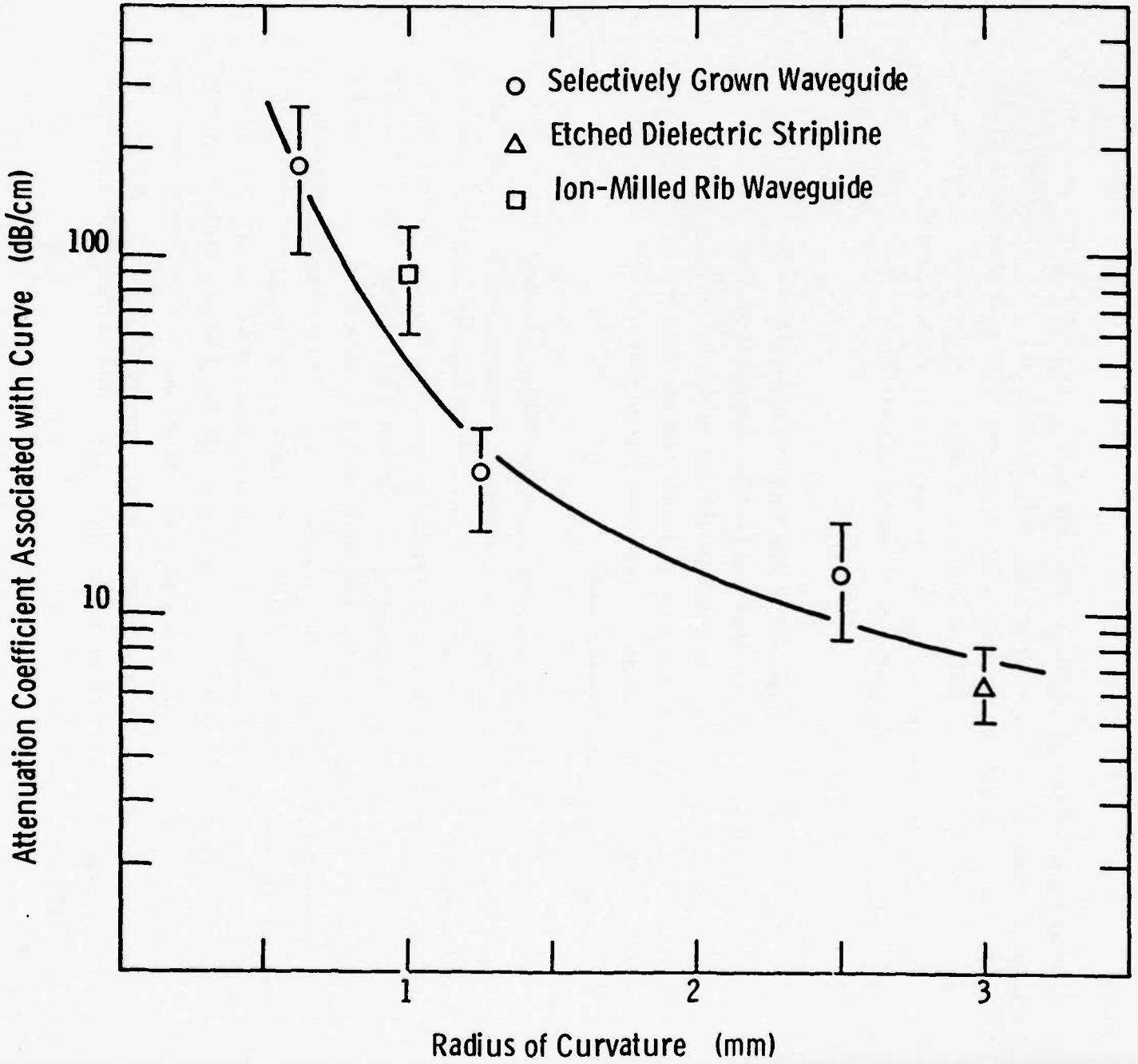

Figure 16 Increase in Attenuation Coefficient Due to the Curved Nature of Bent Waveguides

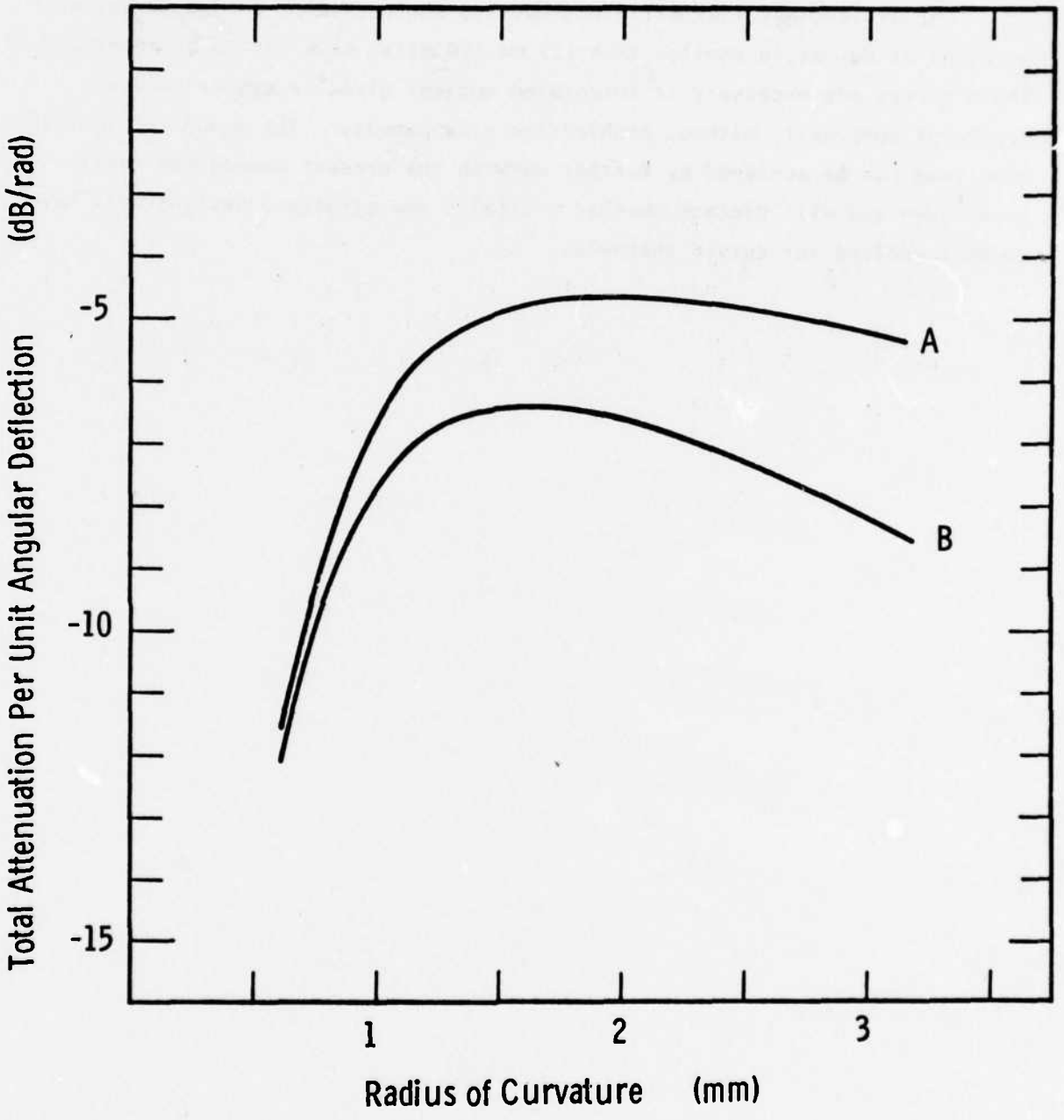

Figure 17 Total Optical Power Attenuation per Unit Angle of Deflection in Curved Waveguides as a Function of Radius of Curvature, Assuming a Straight-Line Attenuation of (A) 10 dB/cm and (B) 20 dB/cm

It is clear that efficient ways to channel light around curves with a radius of curvature smaller than 1.3 mm (50 mils) have yet to be developed. Sharp curves are necessary if integrated optical circuits are to have any degree of complexity without prohibitive size penalty. The amount of improvement that can be achieved by further work on the present waveguides remains to be seen and will dictate whether radically new structure designs will have to be conceived for curved channels.

SECTION IV
(Ga,Aℓ)As ACTIVE DEVICES

Active devices in GaAs waveguides grown by vapor phase epitaxy had been developed previously at Texas Instruments.[9,10] In these devices, electrooptic pads were fabricated by electroplating Schottky barriers on the GaAs surface. Attempts to apply the same technology to LPE-grown (Ga,Aℓ)As surfaces met with serious difficulties traced to the formation of high resistivity interfacial layers between the metal and the semiconductor. Rectifying contacts of SnO_2-doped In_2O_3 on (Ga,Aℓ)As have been reported[11] and constitute one possible answer to the problem. Another solution is the Be^+ ion implantation technique as demonstrated by the GaAs light switches of Leonberger, et al.[12]

The approach we have chosen and demonstrated consists of growing an additional layer of GaAs. Its purpose is to greatly facilitate the fabrication of electroplated Schottky barrier pads. By maintaining the thickness of the GaAs "cap" to small values (less than 3000 Å), the attenuation coefficient at the operating wavelength of a GaAs injection laser is not significantly increased. Both electrooptic directional couplers and single-line modulators have been fabricated using this technique.

A. Electrooptic Directional Coupler/Switch

The basic structure, grown by liquid phase epitaxy (LPE) on (100) GaAs substrates is illustrated in Figure 18. It consists of successive layers of GaAs as a buffer layer, $Ga_{0.85}Al_{0.15}As$ for optical isolation, and $Ga_{0.9}Al_{0.1}As$ as the waveguide. Each layer is 2 to 2.5 μm thick. A final 0.2 to 0.3 μm thick layer of GaAs, which greatly facilitates the electroplating of Pt Schottky barriers, completes the structure. The final layer is kept sufficiently thin to confine the optical field in the $Ga_{0.9}Al_{0.1}As$ layer, thus ensuring that the attenuation will not increase significantly. All the LPE layers are nominally undoped n-type with a carrier density in the mid 10^{15} cm^{-3} range. Figure 19 is an SEM picture of a cleaved and stained cross section of

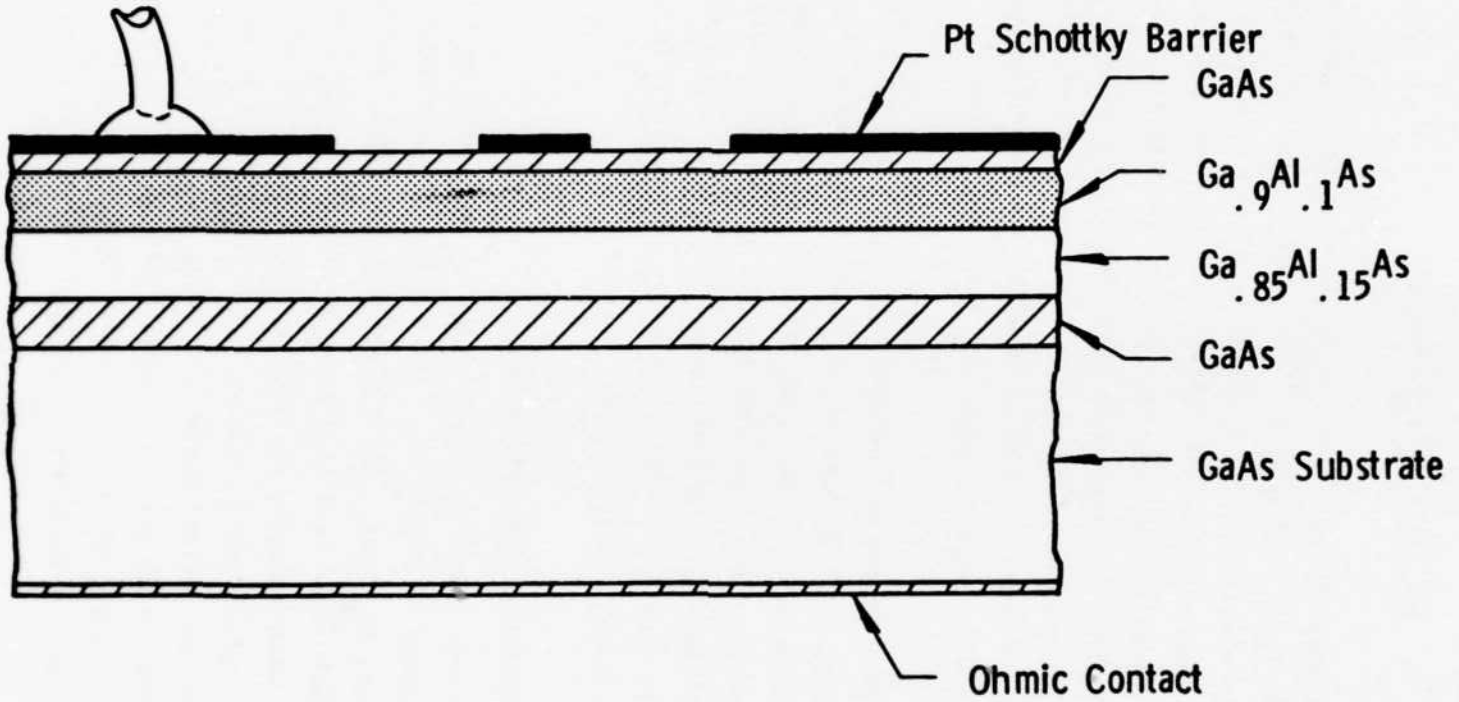

Figure 18 Schematic Configuration of a (Ga,Aℓ)As Electrooptic Directional Coupler Switch

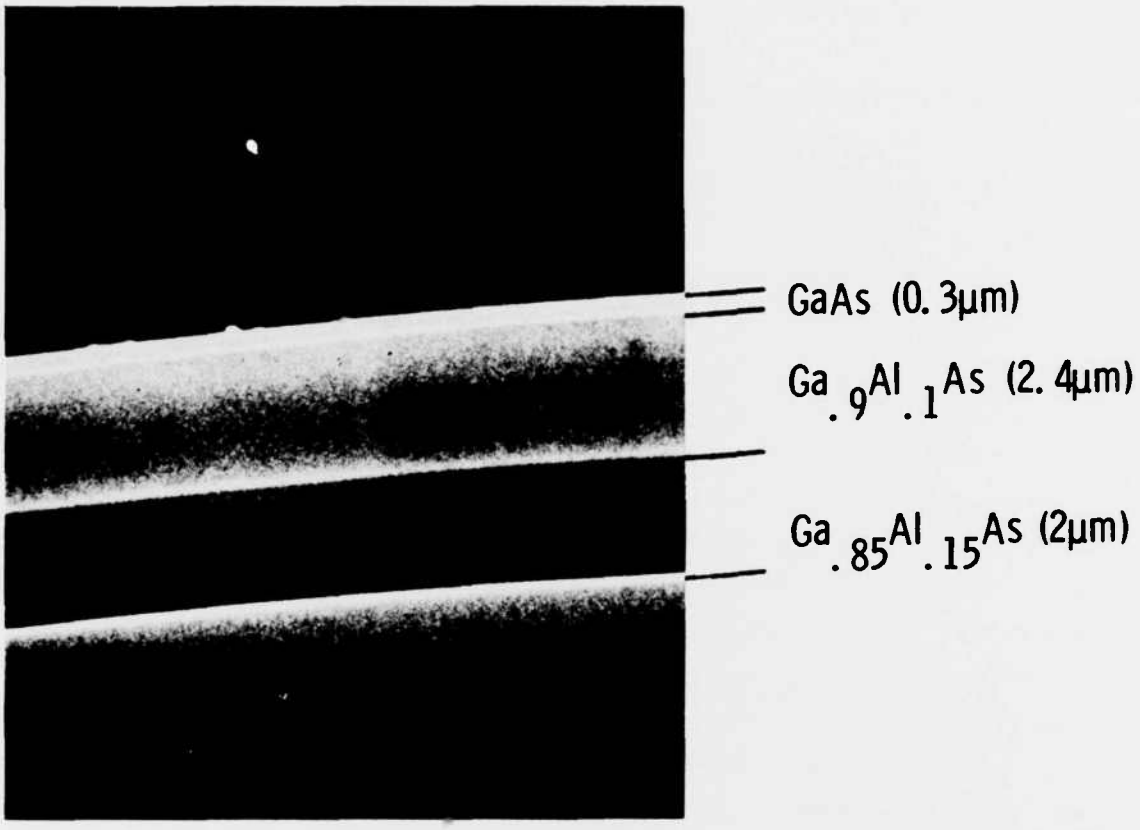

Figure 19 SEM of an Actual (Ga,Al)As EDC Switch. The top GaAs cap is only 3000 A thick.

an actual device. The thickness of the top GaAs is ~ 3000 Å. The underlying $Ga_{0.9}Al_{0.1}As$ waveguide is 2.4 μm thick.

Metal-gap directional couplers were fabricated using the procedure described in Reference 10. The switching characteristics of the resultant device were investigated with a cw Nd:YAG laser. A magnified image of the cleaved exit end of the device was displayed on a TV monitor by means of an infrared-sensitive camera. Figure 20(b) shows that, under passive conditions, approximately 90% of the light fed in the input channel was coupled into the adjacent channel. Each channel was 5 μm wide, with a 5 μm separation, and the interaction length was 8 mm. With a 25 V reverse bias applied to one side of the Schottky barrier switch, crosstalk is inhibited and the light emerges from the input channel, as shown in Figure 20(c). The measured extinction ratio in the coupled channel was in excess of 17 dB at 25 V. Figure 21 shows a more quantitative description of the behavior of the device as a function of applied reverse bias. The overall decreasing trend of total light throughput with increasing reverse voltage, noted by others,[10,12] was observed here. With a contact area of 0.1 x 8.5 mm^2 (4 x 330 $mils^2$), the actual capacitance of the device was 135 pF. This implies a bandwidth of 46 MHz with a 50 Ω load in parallel. For a reduced contact area of 0.013 mm^2 (20 $mils^2$), the projected bandwidth is 2.9 GHz and the power per unit bandwidth would decrease from the present 86 mW/MHz to 1.3 mW/MHz.

The angular divergence of radiation emerging from the cleaved exit face of the device was measured, at λ = 1.06 μm, in a plane perpendicular to that of the layers. The full angular width at half intensity was $\theta = 26°$. This corresponds to the diffraction pattern of a uniformly illuminated slit of width λ/θ = 2.3 μm, in good agreement with the 2.4 μm measured thickness of the waveguide layer. This observation confirms that, even though the GaAs cap has the highest refractive index, the optical energy remains largely confined in the underlying $Ga_{0.9}Al_{0.1}As$ waveguide. By comparing the light

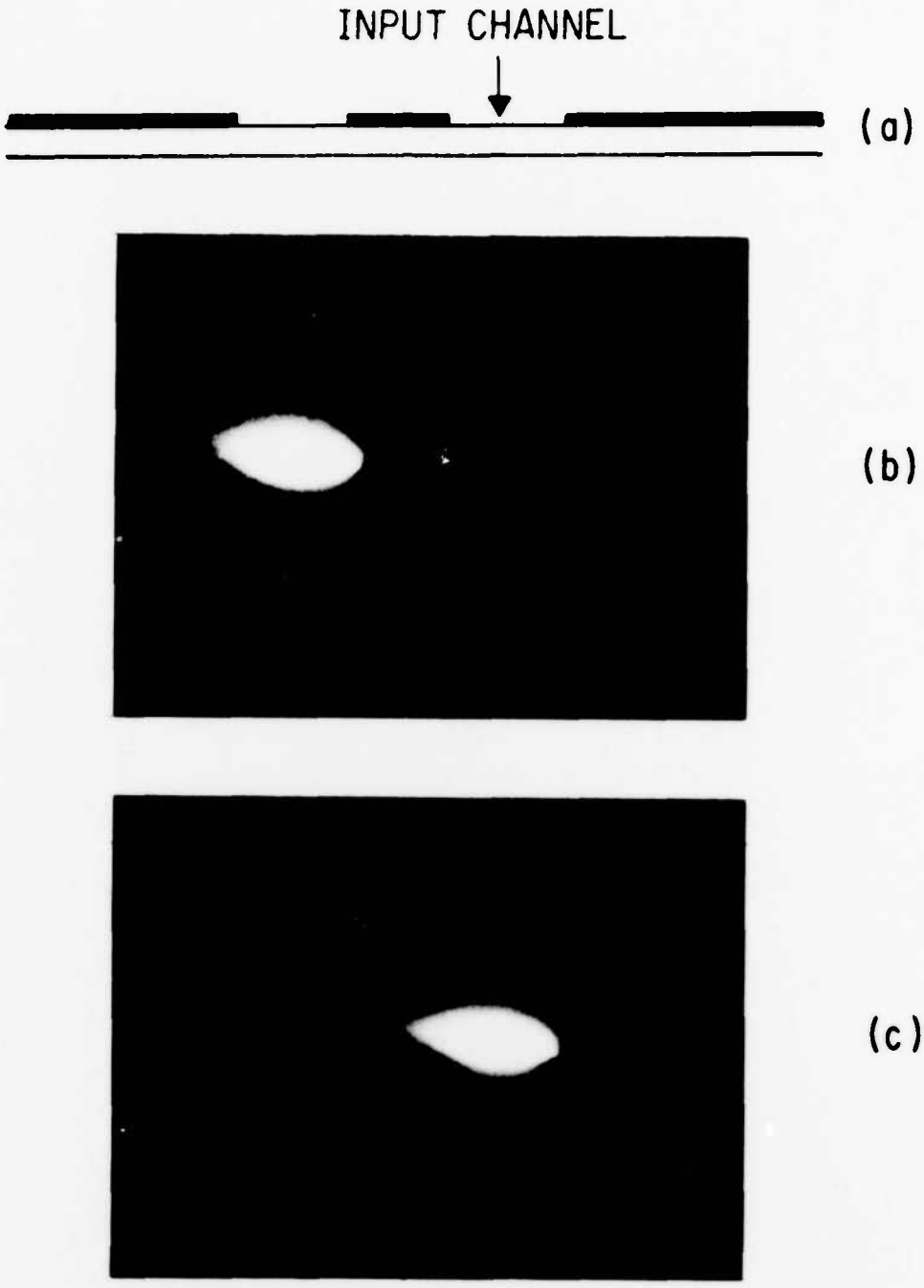

Figure 20 EDC Switch Operating at 1.06 μm. (a) The input channel is on the right. (b) At zero bias, most of the light emerges from the coupled channel. (c) With 25 V reverse bias the light emerges from the input channel.

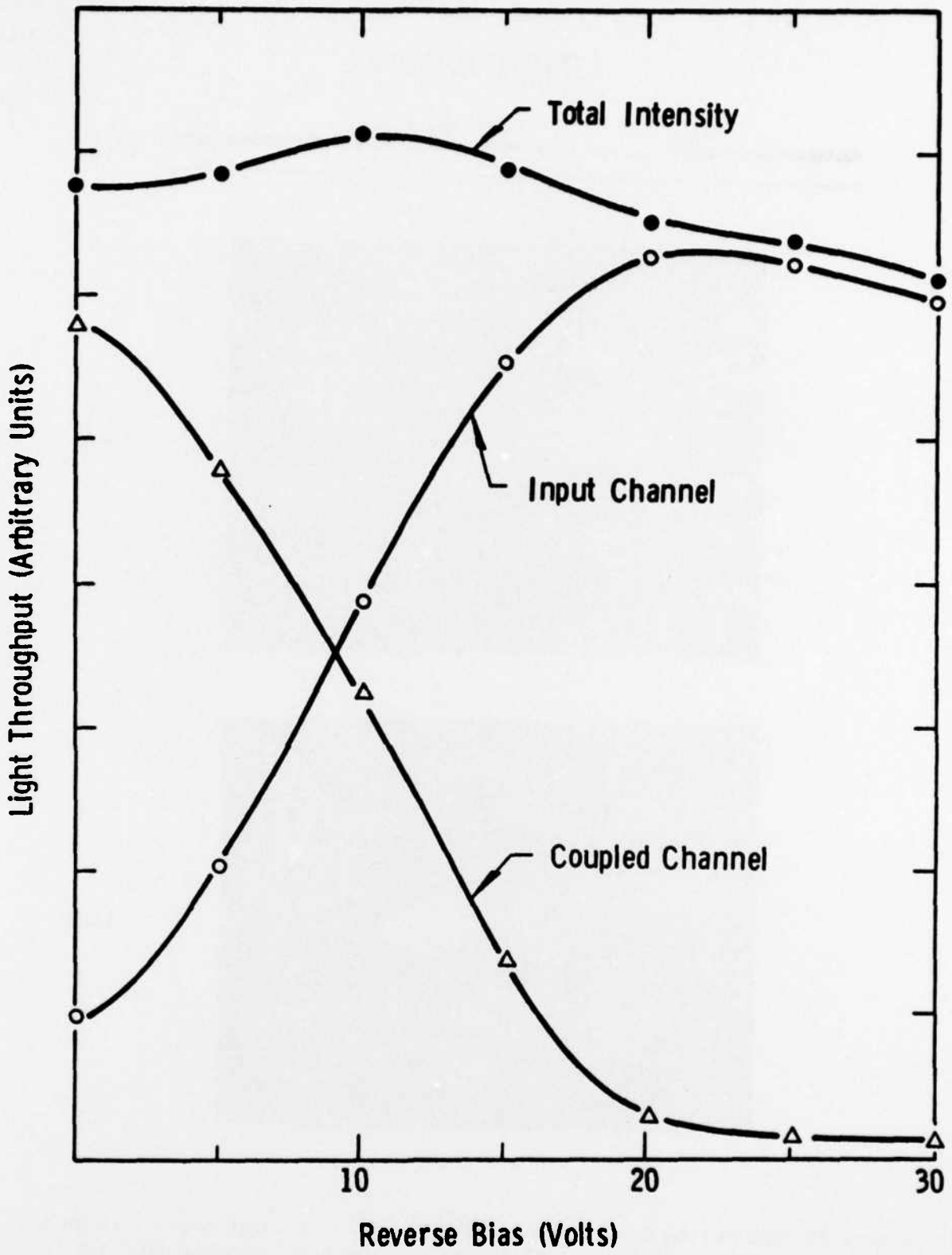

Figure 21 Optical Power Distribution in Input and Coupler Channels of a (Ga,Aℓ)As dc Switch as a Function of Applied Voltage

throughputs using two different sources, namely (1) a cw GaAs laser and (2) our normal cw Nd:YAG laser, we estimate the losses to be about 7 dB/cm at 1.06 μm, and 16 dB/cm at 8600 Å.

B. Single-Line Modulator

The structure of the single-line modulator is illustrated in Figure 22. It is essentially similar to the electrooptic directional coupler-swtich discussed above except that isolated single metal-gap channels are fabricated rather than sets of two closely spaced, adjacent channels.

Single-line channels were defined along mutually perpendicular directions on the same slice, aligned parallel to the [011] and [01$\bar{1}$] cleaved edges, respectively. These two orientations are arbitrarily labeled A and B. Upon reverse biasing one of the two Schottky barriers defining a channel, it was found that the light throughput decreased in type A devices, while it increased in their type B counterparts. Light throughputs as a function of applied reverse bias are shown in Figure 23. The behavior of these devices is related to the crystallographic orientation dependence of the electrooptic properties of GaAs and related compounds. For a [100] slice, and for TE polarized light, the vertical electric field set up by reverse biasing the planar Schottky barriers causes an electrooptically induced change in refractive index which depends on the direction of light propagation. The change "seen" by the light is positive for propagation along the A direction and negative along the B direction.

The refractive index increase seen by light propagating in the A-direction gives rise to a decreasing degree of confinement of the optical power in the metal-gap channel. The field extends farther out underneath the reverse-biased Schottky barrier. Correspondingly, the attenuation associated with the metal cladding increases and the light throughput decreases. The opposite argument prevails for propagation along the B-direction. Thus, the operation

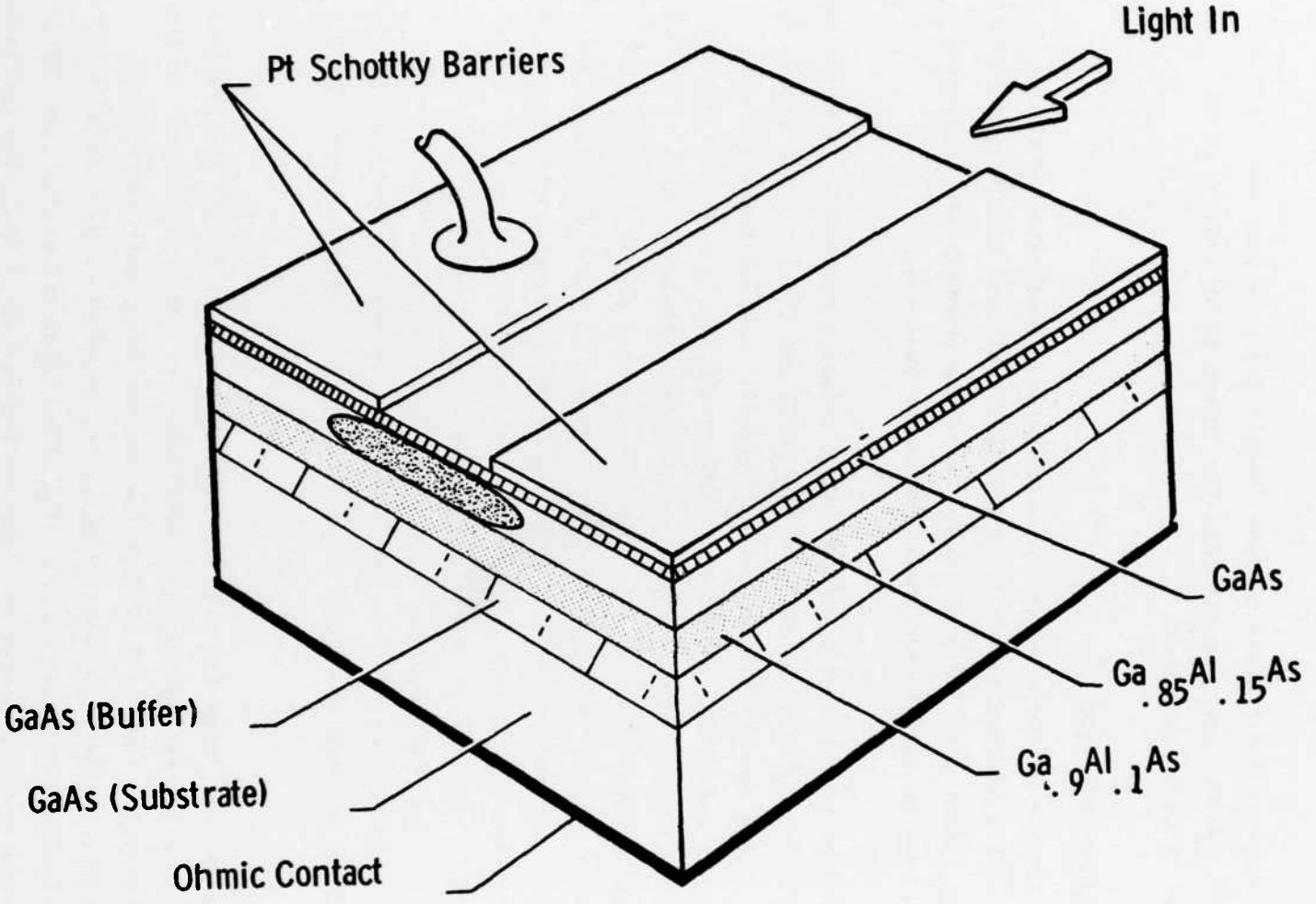

Figure 22 Schematic of a (Ga,Aℓ)As Single-Line Modulator

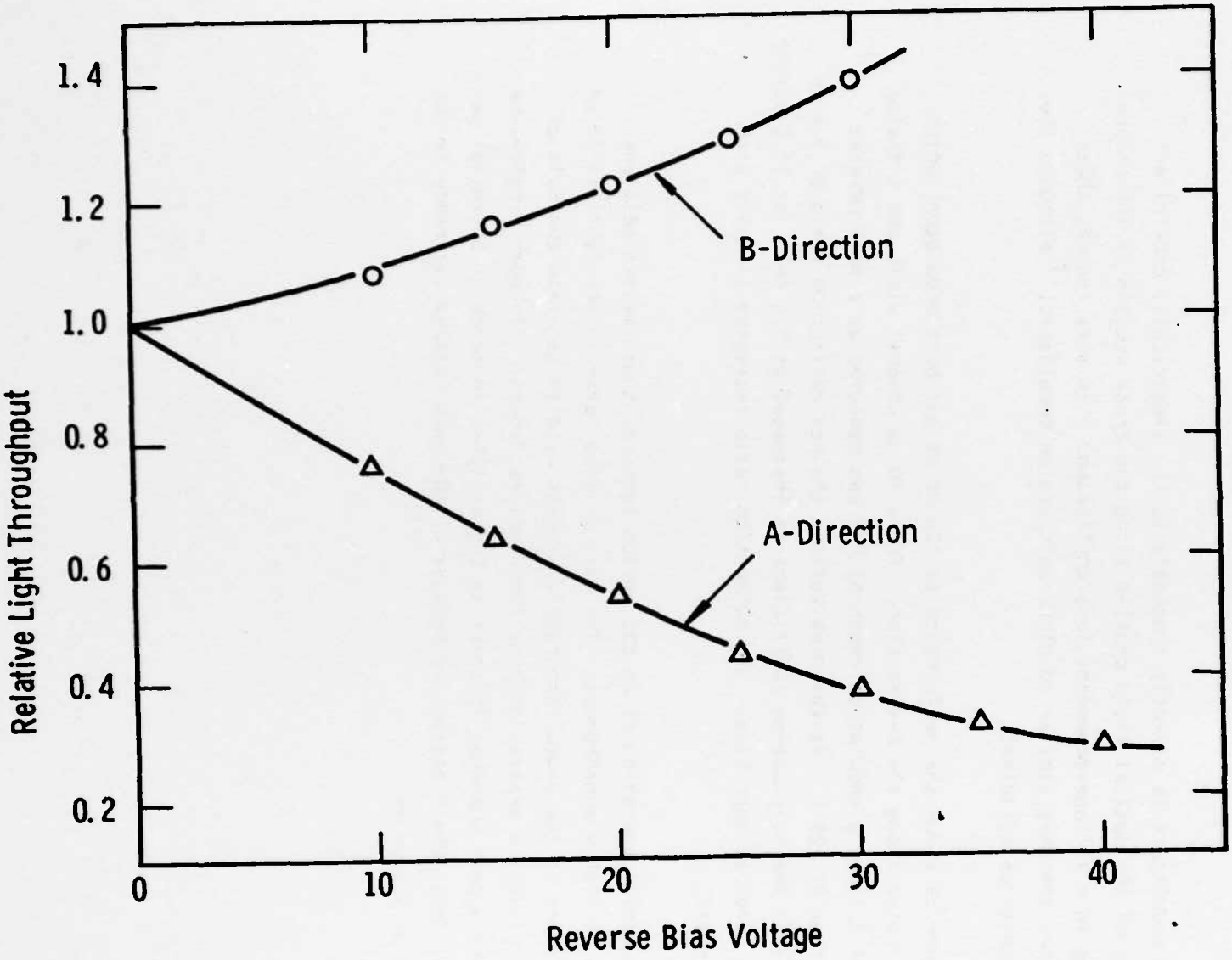

Figure 23 Throughput of TE-Polarized Light in Single-Line Modulators Defined Along the [011] (A) and [01$\bar{1}$] (B) Directions. Device length was 0.7 mm (A) and 0.6 mm (B).

of these modulators is directly traceable to the electrically controlled tailoring of the optical field profile along the cross section of the channel, resulting in a voltage-dependent loss coefficient. In this respect these devices are somewhat similar to electroabsorption modulators,[13] although they are not quite as efficient.

Figure 24 shows the performance at 120 Hz of our best modulator, which was fabricated along the A-direction. For a 10 μm channel width and a device length of 8.5 mm, a modulation depth of 88% was measured at a peak reverse bias voltage of -25 V. At the peak voltage the net extinction ratio of 9.2 dB implies that the attenuation coefficient is increased by 2.5 cm^{-1} (or 10.9 dB/cm) over its value at zero bias. The extinction ratio increases linearly with device length.

Successful operation of an EDC switch requires that the two adjacent channels be highly synchronous. The most critical step in the fabrication of these devices is the photolithographic process used to generate channels of constant width and separation over their entire length. Although single-line modulators appear somewhat inferior to EDC switches in terms of potential performance, they remain attractive because of the much relaxed tolerance in the fabrication procedure.

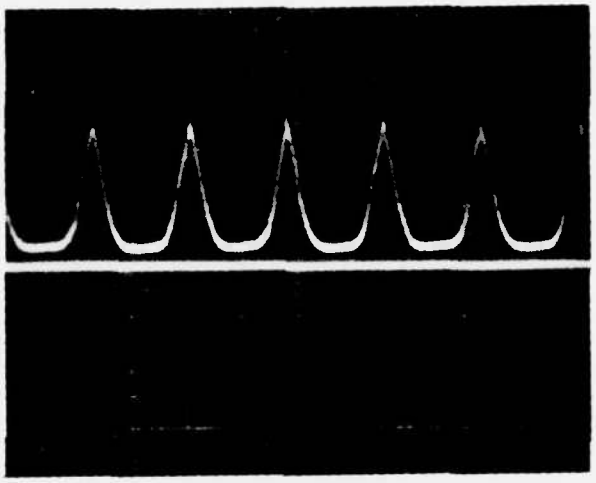

Figure 24 120 Hz Modulation of TE Mode in a 0.85 cm Long Single-Line Modulator in the A Direction. The horizontal trace is the base line.

SECTION V

INTEGRATION OF CURVED WAVEGUIDE WITH MODULATOR

The eletrooptically induced change in refractive index seen by TE waves is maximum positive for propagation along the A direction, maximum negative along the B direction, and zero at 45° with respect to A and B ([001] propagation). This is the reason the output of an I-bar mesa laser, which can be grown only along a [001] direction on a [100] substrate, must be channeled around a 45° curve if it is to be integrated with a modulator/switch.

Because the effective refractive index of a metal-clad waveguide is only slightly lower than that of a similar, but unloaded, planar waveguide, the optical field confinement is generally weak in a metal-gap channel. This is in fact a desirable feature for efficient electrooptic active devices, as the propagation characteristics of a guided wave can be altered electrically only to the extent that the optical field significantly overlaps the region where high electrical fields exist. On the other hand, this very feature makes metal-gap waveguides extremely poor choices to direct light around curves, since this function is best performed in channels with strong optical field confinement.

These mutually contradicting requirements suggest a hybrid approach using dielectric striplines or selectively grown waveguides around curves in conjunction with metal-gap waveguides for modulators and switches. As a vehicle to demonstrate the compatibility between two different types of waveguides, we fabricated and operated the device illustrated in Figure 25. The starting planar structure was similar to the ones used for EDC switches and single-line modulators. A two-step photolithographic process was used. In a first step, the slice was spin-coated with positive photoresist (AZ-1350) and exposed through the 90° curve photomask [see Figure 12(b)] with the straight-line sections blocked off. Development of the photoresist opened up the areas between the curved sections of the channels. Because the waveguiding layer was relatively thick (~ 1.5 μm), it was likely that chemical etching would

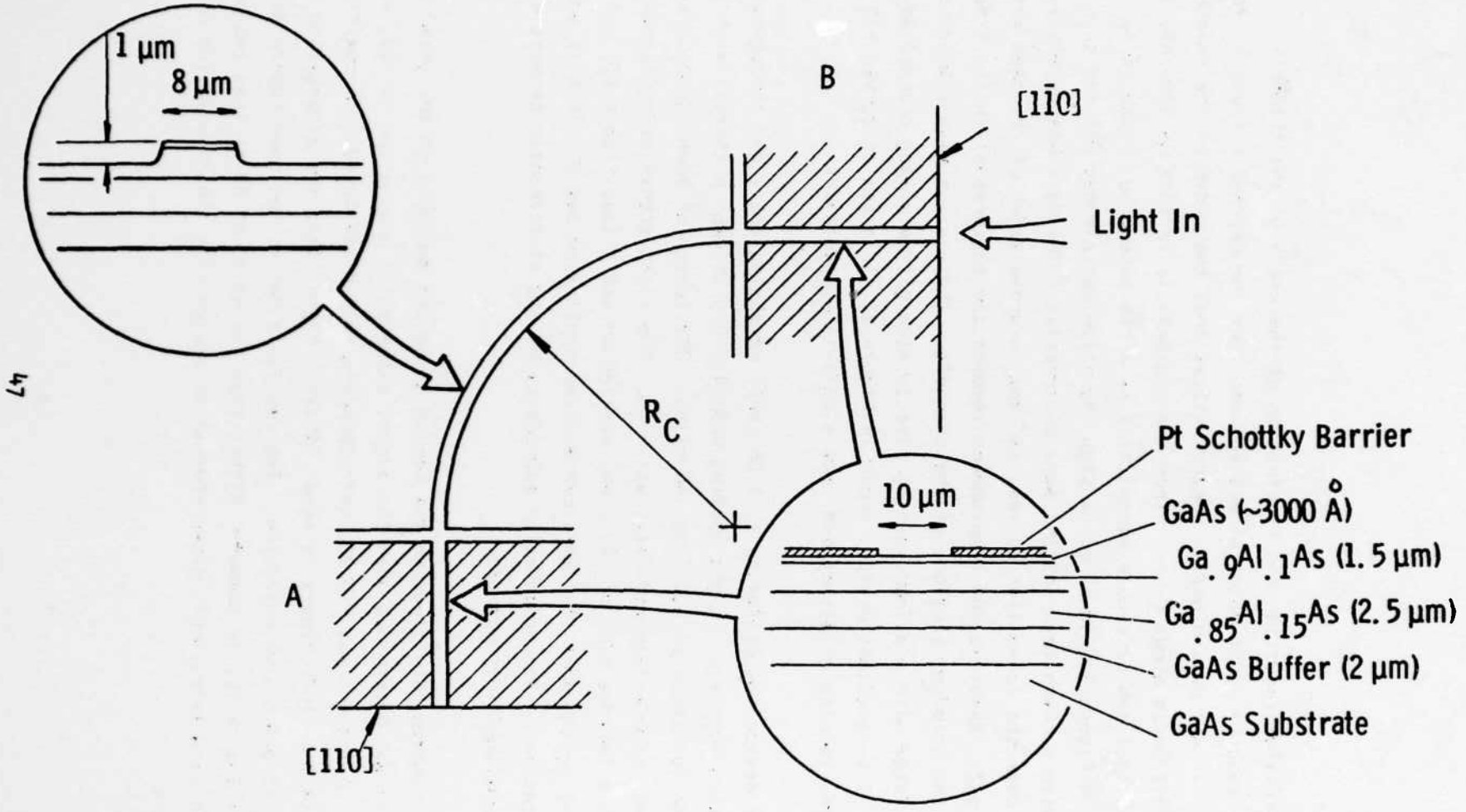

Figure 25 Schematic Configuration of Curved, Ion-Milled Channels Integrated with Single-Line Modulators

cause excessive reduction and fluctuation of the width of the channels. Instead, about 1 μm of material was removed from the exposed surface by ion milling. It was determined on control slices that the width of the channels was at this point about 8 μm. Since the top GaAs is so thin (~ 3000 Å), the curved channel can be viewed essentially as a rib waveguide in the sense defined in Figure 9. In a second step the slice was cleaned off and spin-coated with a fresh layer of the same photoresist. The mask was carefully aligned over the ion-milled curves, and the curved-section of the mask was blocked off. Exposure and development removed the photoresist in the areas between the straight sections of the channels. These areas were subsequently electroplated with platinum, giving rise to stralght metal-gap channel waveguides. The resultant device, shown in Figure 25, is a set of curved rib waveguides feeding at either end into single-line modulators.

The device was evaluated at 1.06 μm by measuring the light throughputs of the various channels. Light guiding was observed through a channel with a radius of curvature of 1.016 mm (40 mils). The length of each straight-section, metal-gap, single-line modulator was 4 mm. The light transmission decreased by [illegible]% when a reverse bias of -40 V was applied on pad A (see Figure 25) and increased by 10% with the same reverse bias applied on pad B. This is another manifestation of the orientation dependence of the electrooptic properties of [100] GaAs/GaAℓAs structures.

By subsequently cleaving the device along the boundary of the metal-clad areas, it was determined that the signal attenuation around the curved, ion-milled rib channel was -17 dB, corresponding to a distributed loss coefficient of 105 dB/cm. This figure is about 90 dB/cm higher than the attenuation of a similar straight-line waveguide. The result, shown as the open square data point in Figure 15, is somewhat higher than the 40 to 60 dB/cm that can be expected in a selectively grown channel waveguide with the same radius of curvature.

While this experiment demonstrates the technical feasibility of integrating curved channel waveguides with metal-gap active devices, it also underscores the need for additional work on structures capable of directing light around curves with substantially lower losses.

SECTION VI
CONCLUSIONS

Significant technological advances were made toward the realization of a practical integrated optical transmitter chip. This progress was brought about by the development of the first truly monolithic double heterojunction GaAs/GaAℓAs laser.

The major accomplishment of the present program was the successful development of efficient (Ga,Aℓ)As modulators and switches compatible with the monolithic 1-bar mesa laser sources. In addition, the ability of various channel waveguide structures to direct light around curves was studied in detail. With present-day technology the optimum radius of curvature is in the 1.3 to 2.5 mm (50 to 100 mil) range for both dielectric striplines and selectively grown waveguides, giving rise to an optical attenuation of at least 5 dB per radian of arc. These numbers must be reduced substantially before integrated optical circuits with any degree of complexity can become reality.

Successful integration of an 1-bar laser with a curved waveguide on the one hand, and of a curved waveguide with a modulator on the other, demonstrates that all three components are compatible for fabrication on a single chip.

REFERENCES

1. J. C. Tracy, W. Wiegman, R. A. Logan, and F. A. Reinhart, Appl. Phys. Lett. 22, 511 (1973).
2. K. L. Lawley, "Monolithic Laser," Report No. ONR-288-016-1F, 30 September 1977, Contract No. N00014-73-C-0288.
3. E. Pinkas, B. I. Miller, I. Hayashi, and P. W. Foy, J. Appl. Phys. 43, 2827 (1972).
4. F. A. Blum, D. W. Shaw, and W. C. Holton, Appl. Phys. Lett. 25, 116 (1974).
5. E. A. J. Marcatili, Bell Syst. Tech. J. 48, 2103 (1969).
6. H. Furuta, H. Noda, and A. Ihaya, Appl. Opt. 13, 322 (1974).
7. V. Ramaswany, Bell Syst. Tech. J. 53, 694 (1974).
8. J. K. Butler, C. S. Wang, and J. C. Campbell, J. Appl. Phys. 47, 4033 (1976).
9. J. C. Campbell, F. A. Blum, and D. W. Shaw, Appl. Phys. Lett 26, 640 (1975).
10. J. C. Campbell, F. A. Blum, D. W. Shaw, and K. L. Lawley, Appl. Phys. Lett. 27, 202 (1975).
11. F. K. Reinhart, W. R. Sinclair, and R. A. Logan, Appl. Phys. Lett. 29, 21 (1976).
12. F. J. Leomberger, J. P. Donnelly, and C. O. Bozler, Appl. Phys. Lett. 29, 652 (1976).
13. G. E. Stillman, C. M. Wolfe, C. O. Bozler, and J. A. Rossi, Appl. Phys. Lett. 28, 544 (1976).

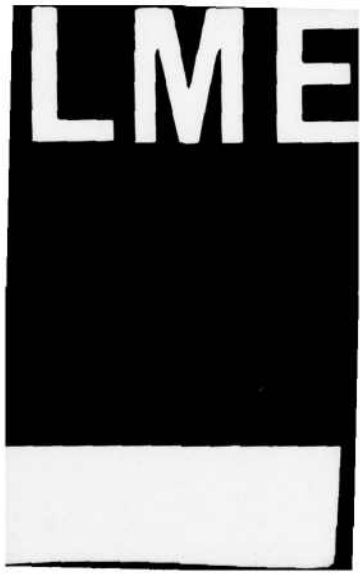
LME